ARMY RESEARCH LABORATORY

Detection of Energetic Materials and Explosive Residues With Laser-Induced Breakdown Spectroscopy: I. Laboratory Measurements

by Jennifer L. Gottfried, Frank C. De Lucia Jr., Russell S. Harmon, Chase A. Munson, Raymond J. Winkel, Jr., and Andrzej W. Miziolek

ARL-TR-4240 **September 2007**

NOTICES

Disclaimers

The findings in this report are not to be construed as an official Department of the Army position unless so designated by other authorized documents.

Citation of manufacturer's or trade names does not constitute an official endorsement or approval of the use thereof.

Destroy this report when it is no longer needed. Do not return it to the originator.

Army Research Laboratory
Aberdeen Proving Ground, MD 21005-5066

ARL-TR-4240 **September 2007**

Detection of Energetic Materials and Explosive Residues With Laser-Induced Breakdown Spectroscopy: I. Laboratory Measurements

Jennifer L. Gottfried, Frank C. De Lucia Jr., Russell S. Harmon, Chase A. Munson, Raymond J. Winkel, Jr., and Andrzej W. Miziolek
Weapons and Materials Research Directorate, ARL

REPORT DOCUMENTATION PAGE

Form Approved
OMB No. 0704-0188

1. REPORT DATE *(DD-MM-YYYY)*	2. REPORT TYPE	3. DATES COVERED (From - To)
September 2007	Final	October 2002–April 2007

4. TITLE AND SUBTITLE
Detection of Energetic Materials and Explosive Residues With Laser-Induced Breakdown Spectroscopy: I. Laboratory Measurements

5a. CONTRACT NUMBER

5b. GRANT NUMBER

5c. PROGRAM ELEMENT NUMBER

6. AUTHOR(S)
Jennifer L. Gottfried, Frank C. De Lucia Jr., Russell S. Harmon, Chase A. Munson, Raymond J. Winkel, Jr., and Andrzej W. Miziolek

5d. PROJECT NUMBER
622618H8049

5e. TASK NUMBER

5f. WORK UNIT NUMBER

7. PERFORMING ORGANIZATION NAME(S) AND ADDRESS(ES)
U.S. Army Research Laboratory
ATTN: AMSRD-ARL-WM-BD
Aberdeen Proving Ground, MD 21005-5066

8. PERFORMING ORGANIZATION REPORT NUMBER
ARL-TR-4240

9. SPONSORING/MONITORING AGENCY NAME(S) AND ADDRESS(ES)

10. SPONSOR/MONITOR'S ACRONYM(S)

11. SPONSOR/MONITOR'S REPORT NUMBER(S)

12. DISTRIBUTION/AVAILABILITY STATEMENT
Approved for public release; distribution is unlimited.

13. SUPPLEMENTARY NOTES

14. ABSTRACT
Laser-induced breakdown spectroscopy (LIBS) has been investigated for the detection of energetic materials. After an initial survey of explosives and propellants, key elemental and molecular emission lines in the LIBS spectra were identified. Techniques for improving the sensitivity and selectivity of LIBS for explosives detection, such as the use of an argon buffer gas and double pulse LIBS, have been investigated with laboratory and field-portable instruments. We present results demonstrating the ability of LIBS to discriminate between energetic and non-energetic materials.

15. SUBJECT TERMS
explosive detection, LIBS

16. SECURITY CLASSIFICATION OF:			17. LIMITATION OF ABSTRACT	18. NUMBER OF PAGES	19a. NAME OF RESPONSIBLE PERSON
a. REPORT	b. ABSTRACT	c. THIS PAGE			Jennifer L. Gottfried
UNCLASSIFIED	UNCLASSIFIED	UNCLASSIFIED	UL	42	19b. TELEPHONE NUMBER (*Include area code*) 410-306-0884

Standard Form 298 (Rev. 8/98)
Prescribed by ANSI Std. Z39.18

Contents

List of Figures

List of Tables

1. Introduction

1.1 Background

The direct chemical detection of energetic materials and explosive residues in real time is a particularly challenging problem. Interest in overcoming the difficulties associated with the detection of explosives has grown over the past decade and is now shared by many Government organizations. The military has a vital interest in the development of field-portable sensors to detect land mines, improvised explosive devices, remotely detonated munitions, hidden armaments, and unexploded ordnance. Homeland security requires an analytical capability for the detection of trace amounts of explosives or their residues in a variety of different situations (e.g., in airplane, train, or ship passenger luggage, in vehicles, and within transport containers). Also, the ability to detect trace amounts of explosive residues would greatly benefit forensic investigations of destructive explosive events.

Energetic and explosive materials are pure substances or mixtures that chemically react to rapidly liberate large amounts of heat and gas. Today, about 150 different formulations are used in military, commercial, and illicit manufacture of explosives (*1*). Energetic materials and explosives may be inorganic or organic in nature and can be divided into two broad categories (low-energy explosives and high-energy explosives) based on factors related to how readily a reaction is initiated and its intensity. Many explosives consist of a fuel component (usually a hydrocarbon) and an oxidizer (typically an oxide of nitrogen), which may be contained within the same molecule (*1*). To be of broad utility, a sensing technique would need to have the capability to rapidly detect and identify the wide variety of different constituents that are present in energetic materials and explosives.

Although some methods for detecting bulk explosives such as x-ray analysis, neutron activation or scattering (which measures quantities of carbon, nitrogen, and oxygen) (*2*), and terahertz imaging are currently used or undergoing development, many of these systems are quite large and expensive. One of the most pressing needs for the military is the stand-off detection of explosives. As a result of drastically reduced sensitivity at increasing distances and the generation of potentially harmful ionization radiation, neither x-ray imaging nor neutron activation is practical at stand-off distances (*3*). Although terahertz imaging is a promising technique that employs non-ionizing radiation, absorption of water vapor and other species in the atmosphere could potentially limit its application to stand-off detection (*4*, *5*).

Most trace explosive detection techniques, such as ion mobility spectrometry and gas chromatography, rely on vapor detection. Unfortunately, at room temperatures, the vapor pressures of many common explosives are extremely small (ppb_v or less), and attempts to conceal the explosives by sealing them in packaging materials can decrease the vapor

concentrations by as many as three orders of magnitude (*6*). A single first generation C-4 fingerprint, however, can contain several milligrams of hexahydro-1,3,5-trinitro-s-trazine (RDX) (*7*). Optical techniques such as cavity ringdown spectroscopy (CRDS), Raman spectroscopy, photoacoustic spectroscopy, and photofragmentation followed by resonance-enhanced multiphoton ionization (PF-REMPI) or laser-induced fluorescence (PF-LIF) have been applied to trace explosive detection (*5*). Of these techniques, only Raman has been demonstrated on solid explosives at stand-off distances (10 to 50 m), although long integration times (i.e. multiple laser shots) were required to improve the signal-to-noise ratio (*8, 9*).

An alternate optical technique for the detection of explosives is laser-induced breakdown spectroscopy (LIBS). LIBS is a spectroscopic analysis technique that uses the light emitted from a laser-generated microplasma to determine the composition of the sample, based on elemental and molecular emission intensities. The ability of LIBS to provide remote, rapid multi-element micro-analysis of bulk samples (solid, liquid, gas, aerosol) in the parts-per-million range with little or no sample preparation has been widely demonstrated (*10*) and is the greatest advantage of LIBS compared with other analytical approaches. LIBS holds particular promise for the detection and identification of explosives because of its intrinsic capability for minimally destructive, *in situ*, real-time detection and analysis of chemical species.

LIBS has the following properties: (a) it is a simple and straightforward technique; (b) no sample preparation is required; (c) it is very sensitive, e.g., only a very small sample is required (nanograms–picograms) for production of a usable LIBS spectrum; (d) it is fast, providing real-time (<1 s) response; (e) LIBS sensors can be made rugged and field portable; (f) all components (i.e., laser, detector, computer, etc.) can be miniaturized; and (g) LIBS offers the flexibility of point detection or operation in a stand-off mode. With recent advances in broadband detectors (multispectrometer or echelle), LIBS is now capable of detecting a wide variety of toxic and hazardous compounds. No other sensor is capable of detecting all classes of chemical compounds and all types of matter. Researchers at the U.S. Army Research Laboratory (ARL) have previously used LIBS for the detection of Halon alternative agents (*11*), tested a field-portable LIBS system for the detection of lead in paint (*12*), and demonstrated the detection of chemical and biological warfare agent surrogates (*13–16*). Here, we report recent results for the detection of energetic materials and explosive residues under close-contact laboratory conditions. An ensuing report (*17*) will detail the extension of these results to the stand-off detection of explosive residues with the use of LIBS.

1.2 LIBS of Explosives

In the past, LIBS has been primarily used to analyze one or a few elements, mostly metals (*10*). More recently, the capability of LIBS to identify compounds has been realized with the advent of high-resolution broadband spectrometers. Every element on the periodic table has characteristic atomic emission lines that emit in the visible spectrum. A broadband spectrometer allows one to capture all the elements in the sample interrogated by the laser-generated plasma, provided they

are present in sufficient abundance. Instead of concentrating on a small portion of a LIBS spectrum as with a Czerny-Turner type monochromator, all the emitting elements in a sample can be observed in a full broadband LIBS spectrum. LIBS can more readily be applied to a variety of materials beyond metals, including plastics and other organic materials, biological materials, and other hazardous compounds.

The carbon, hydrogen, oxygen, and nitrogen atomic emission lines (which span the ultraviolet to near infrared regions) are commonly used to identify organic compounds. Anzano et al. (*18*) used LIBS to see if linear correlation techniques would allow sorting of a variety of plastics, including polystyrene and high-density polyethylene. Subtle differences in the carbon and hydrogen intensities enabled successful identification 90% to 99% of the time. Portnov et al. (*19*) used LIBS to investigate the spectral signatures of nitroaromatic and polycyclic aromatic hydrocarbon samples. They observed the atomic emission lines associated with C, H, N, and O, but they also observed emission attributable to molecular fragments associated with the CN ($B^2\Sigma^+$–$X^2\Sigma^+$) violet system and the C_2 ($d^3\Pi_g$–$a^3\Pi_u$) Swan system. These fragments were used to successfully show differences between the compounds studied. Ferioli and Buckley (*20*) have used LIBS to study hydrocarbon mixtures (C_3H_8, CH_4, and CO_2 in air). The strength of the C, N, and O atomic emission lines was investigated in relation to the concentration of carbon and hydrogen in the samples.

In addition to the absolute intensities of the atomic emission lines, the peak intensity ratios of these lines have been used to analyze samples. Tran et al. (*21*) analyzed the atomic intensity ratios of several organic compounds in order to determine the empirical formula of a compound, based on the ratios from several elements. Calibration curves were built, based on C:H, C:O, and C:N atomic emission ratios, from a variety of compounds that covered a wide range of stoichiometries. Four compounds with known stoichiometries were tested against the calibration curves. The ratios determined from the calibration curves were compared with the actual stoichiometries and showed an accuracy of 3% on average. In the study of nitro-aromatic and polycyclic aromatic hydrocarbon samples described previously, the ratios between C_2 and CN and between O and N of different samples were shown to correlate with the molecular formula (*19*). Anzano et al. also attributed the success of their correlation of plastics to differences in the C/H atomic emission intensity ratio of each sample (*18*).

Recent efforts at ARL have focused on optimizing the sensitivity and selectivity of LIBS for the detection of explosive residues. The ability of LIBS to detect trace amounts of materials with a single laser shot is especially important for residue detection, since the first shot can ablate all or most of the residue. The success of LIBS for identifying organic compounds, based on atomic emission intensity ratios, led researchers at ARL to investigate characteristics of LIBS spectra of explosive compounds. Carbon, hydrogen, oxygen, and nitrogen are found in most military explosives. A common characteristic of most explosives is their high nitrogen and oxygen content relative to the amount of carbon and hydrogen (*22*). By tracking the amounts of oxygen and nitrogen in a sample relative to the other elements, it is possible to determine if a compound

is energetic or non-energetic (*23*). Figure 1 shows the molecular formulas or structures of several explosives and potential interferents. The interferents have a much higher carbon and hydrogen content relative to the oxygen and nitrogen than the explosives. Some of the interferents contain no nitrogen at all; however, the oxygen content is still low relative to hydrogen and carbon. Furthermore, diesel fuel is a combination of chains of hydrogen and carbon with no oxygen or nitrogen content. These differences can be exploited with LIBS in order to improve discrimination between energetic and non-energetic materials.

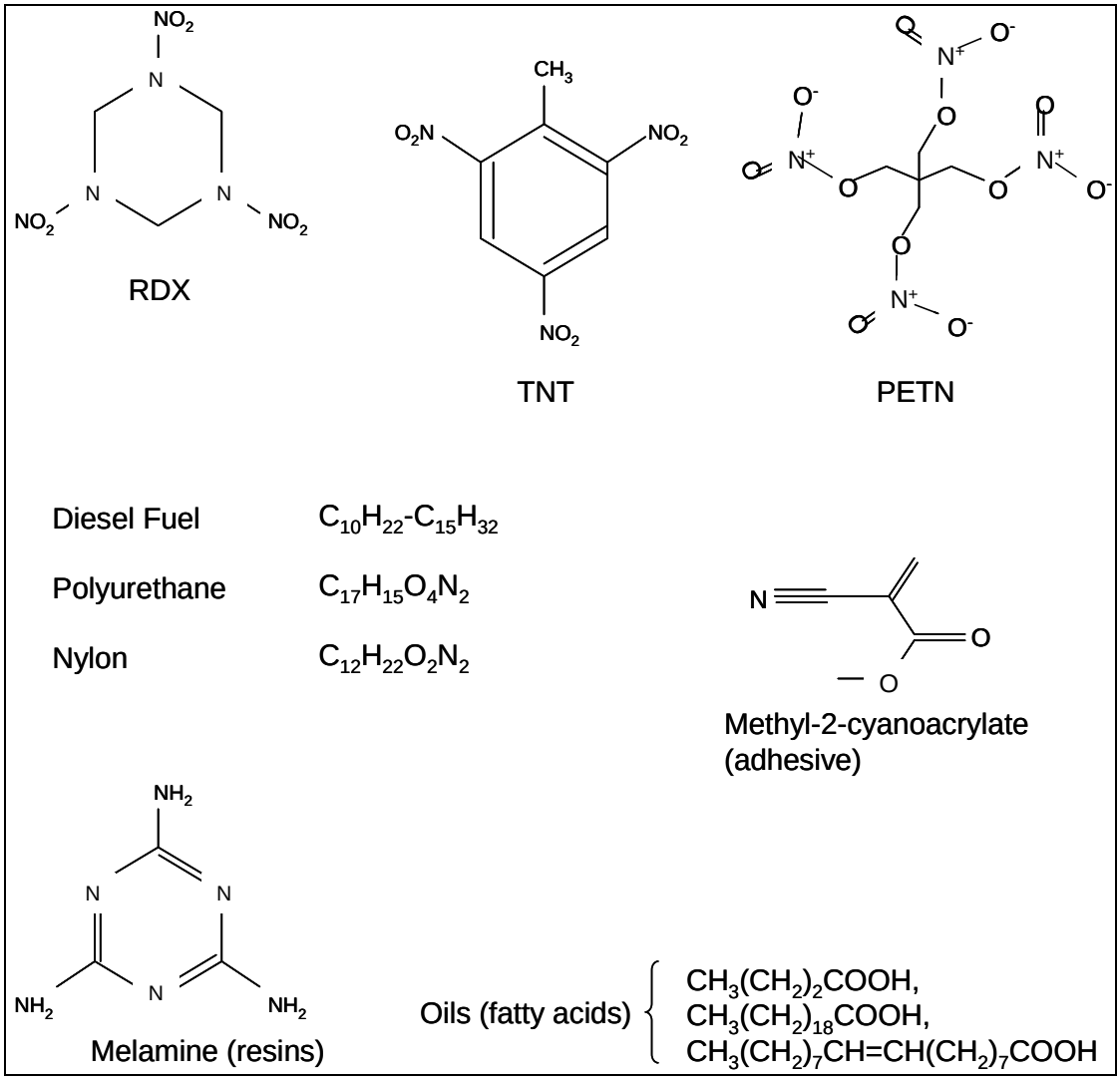

Figure 1. Structures or formulas of several explosives and non-energetic organic compounds.

Although explosive residues can be identified, based on the elemental ratios of carbon, hydrogen, nitrogen and oxygen, entrainment of atmospheric oxygen and nitrogen into the laser-induced plasma complicates the discrimination of energetic and non-energetic materials. Minimizing the oxygen and nitrogen contribution from the atmosphere is necessary to track the true value of oxygen and nitrogen relative to carbon and hydrogen in a LIBS spectrum. The formulation of

RDX, for example, has equal amounts of O and N. Air alone has more nitrogen (80%) relative to oxygen (20%). Eliminating the nitrogen and oxygen contribution from air therefore results in a larger O:N ratio characteristic of an explosive material (*24*).

1.3 Complications in the LIBS Spectra Because of Air

In a laboratory setting, argon can be used to displace the ambient atmosphere from the surface of the sample. As an added benefit, the use of argon as a buffer gas at atmospheric pressures also results in an increase in emission signal compared to air (*25*). Although we demonstrate in this report that using an inert gas to displace the air above the sample is effective for close-contact studies, it cannot practically be used for stand-off applications (*17*). Alternatively, multiple laser pulses can be used to interrogate the sample. We have used double pulse LIBS to reduce the amount of air entrained in the laser-induced plasma and improve the discrimination of energetic and non-energetic materials.

In double pulse LIBS, two successive laser pulses are used to generate the microplasma. Typically, the laser pulses are separated by a few microseconds. Researchers have used a variety of double pulse LIBS experimental configurations ranging from collinear nanosecond laser pulses to orthogonal laser sparks using both a femtosecond pulse and a nanosecond pulse (*26–31*). The main advantage of double pulse LIBS for most applications is the observed increase in signal; consequently, studies of double pulse LIBS have increased in recent years (*31*). The extent of the reported signal increases depends on many factors, including pulse separation times, wavelength, pulse energies, sample, and experimental configuration. Another advantage of using two pulses is that the ablation pulse is separate from the analytical pulse, thus improving reproducibility in most cases. Since we are ultimately concerned with performing LIBS stand-off experiments, all our laboratory double pulse LIBS experiments were performed with two collinear pulses.

A combination of several factors is thought to increase the emission signal in double pulse LIBS. These factors include greater mass ablation, larger plasma volume (more atoms are excited), and less laser shielding of the second pulse, which results from the decrease in gas density after the first pulse (*28–31*). When the first laser pulse hits, it impacts the sample and displaces the surrounding gas. The second pulse arrives and interacts with the material within the first plasma in a reduced density environment. We have attempted to exploit the decrease in gas density for explosives detection. The decrease of surrounding air density within the analytical (second) plasma should diminish the influence of oxygen and nitrogen from the atmosphere on the LIBS emission signals. The oxygen and nitrogen signal obtained will be more representative of the sample composition than the surrounding air; thus, a better determination of whether an unknown material is an explosive can be achieved.

2. Experimental

A standard laboratory LIBS system is shown in figure 2. The basic LIBS setup consists of a pulsed laser (typically the fundamental of a Nd:YAG* laser 1064 nm, 8-ns pulse width), optics for focusing the laser and light collection from the laser-induced microplasma, a spectrograph for dispersing the collected emission, and a computer for recording and analyzing the LIBS spectrum. The focused laser pulse ablates a small amount of the sample material and dissociates the resulting molecules and particulates within the plasma volume. For a typical setup the laser power at the focal point is >1 GW/cm^2 in order to produce a microplasma. The subsequent emission can be resolved spectrally and temporally in order to generate a spectrum containing emission lines from the atomic, ionic, and molecular fragments created by the plasma. A single laser event and subsequent data analysis can take place in less than a second.

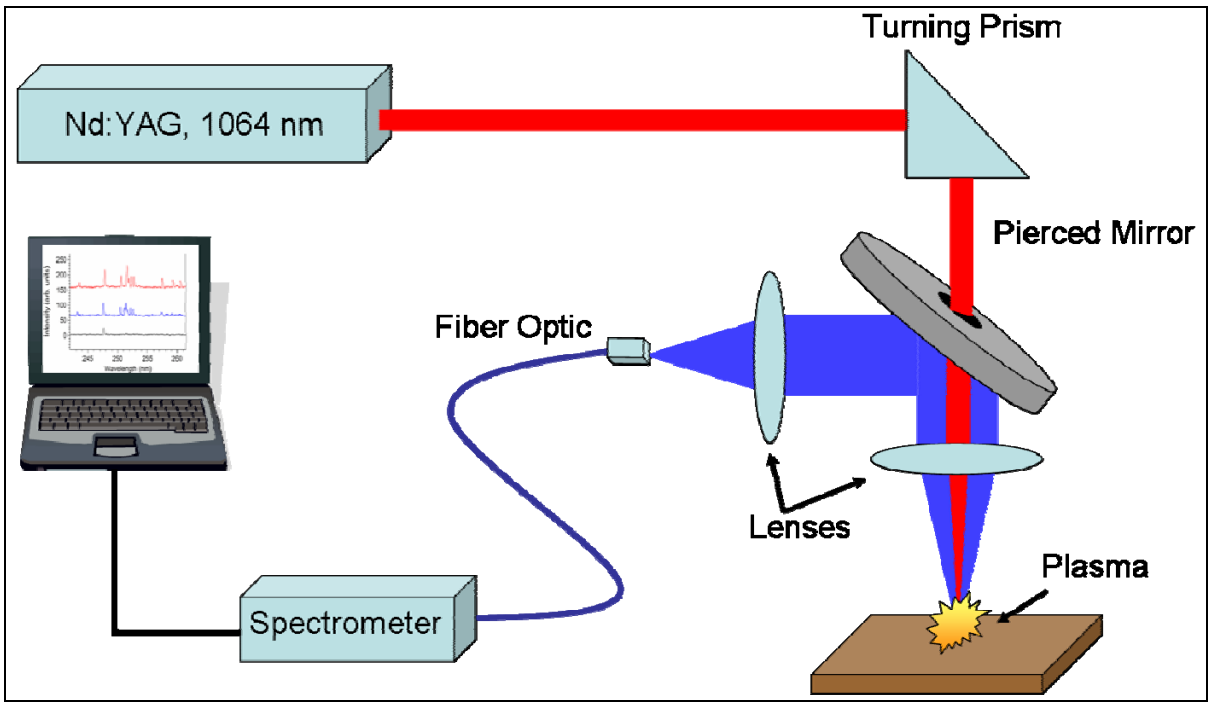

Figure 2. Basic LIBS experimental setup. (The laser is fired, passed through a turning prism and pierced mirror, and is focused on the sample surface to induce a microplasma. The resulting light emission characteristic of the sample composition is focused into a fiber optic and dispersed with a spectrograph to obtain the LIBS spectrum.)

Because of the simplicity, compactibility, and ruggedness of the instrumentation, a wide range of sensors based on LIBS has been developed by various groups over the years. Figure 3 illustrates some of the different LIBS applications and configurations that have been envisioned.

*Nd:YAG = neodymium-doped yttrium aluminum garnet.

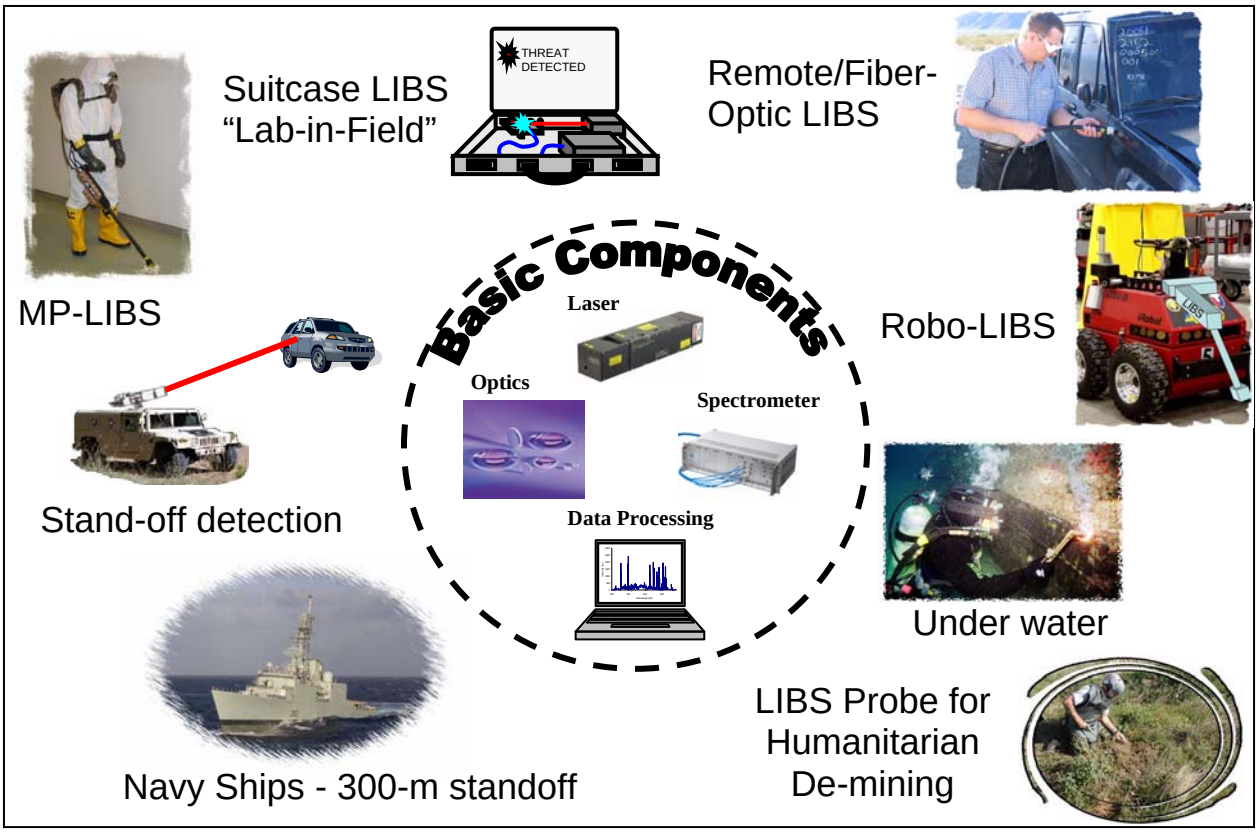

Figure 3. LIBS sensor suite and applications. (The basic LIBS components are compactible and ruggedizable and have been configured by different groups for a variety of applications.)

A number of LIBS systems have been developed by ARL and used to obtain spectra of energetic materials and residues. The following paragraphs describe the laboratory systems used in this research, as well as specialized instrumentation for portable applications.

One of the earliest laboratory LIBS systems at ARL uses the pulse (~10 ns, 30 mJ) from an actively *Q*-switched Nd:YAG laser (Ultra Big Sky Laser) focused by a 50-mm convex lens onto a sample (*24*). A bundle of seven fibers (diameter, 600 μm) collects the emission from the plasma spark. A lens (Ocean Optics, Inc.) is placed in front of the fiber bundle so that the plasma spark is sufficiently defocused for each fiber to collect the same emission and to eliminate any spatial effects. Each of the fibers is connected to an individual high-resolution (0.1-nm) broadband spectrometer (Ocean Optics, Inc., LIBS2000+). Each spectrometer covers a different segment of the 200- to 980-nm spectral range of the LIBS system. Thus, we are able to observe all constituents of an energetic or explosive material. All LIBS spectra with this system were collected with a 1.5-μs delay to eliminate plasma continuum effects. The detectors remained open for 2 ms. The LIBS spectra collection software and the LIBS library software were provided by Ocean Optics, Inc.

We surveyed a variety of energetic and explosive materials with the broadband LIBS2000+ system. Initially, we investigated black powder and its typical components: charcoal, potassium nitrate, calcium sulfate, ammonium nitrate, and sulfur, with no sample preparation. Subsequently, we investigated several pure organic energetics: RDX, octahydro-1,3,5,7-tetrocine (HMX), pentaerythrite tetranitrate (PETN), nitrocellulose (NC), and 2,4,6-trinitrotoluene (TNT), which had been prepared by dissolution into acetone and subsequent evaporation of the pure organic onto glass slides. We pre-treated these samples to get the purest possible LIBS spectrum for each explosive for use as a baseline comparison with explosives that had been handled or mixed into operational formulations. We also studied several operational explosives and propellants: C-4, M-43, LX-14, JA2, and A-5. The chemical compositions of all the explosive materials examined in our initial survey with the LIBS2000+ system are listed in table 1. The operational explosives and propellants contain a diverse suite of different binders and plasticizers.

Table 1. Explosives and energetic materials.

Sample (Type)	Composition
RDX (explosive)	Hexahydro-1,3,5-trinitro-s-trazine
HMX (explosive)	Octahydro-1,3,5,7-tetrocine
TNT (explosive)	Trinitrotoluene
PETN (explosive)	Pentaerythritol tetranitrate
NC (propellant)	Nitrocellulose
C-4 (explosive)	91% RDX, 9% plasticizer [5.3% di(2-ethylhexyl)sebacate, 2.1% polyisobutylene, 1.6% motor oil]
M-43 (propellant)	76% RDX, 4% nitrocellulose, 12% cellulose acetate/butyrate, 8% plasticizer, <1% additives
LX-14 (propellant)	95.5% HMX, 4.5% estane
JA2 (propellant)	60% nitrocellulose, 15.8% nitroglycerine, 25.2% plasticizer [diethylene glycol dinitrate], 0.74% Akardite II [*N*-methyl-*N*,*N*'-diphenyl urea (burning rate moderator and stabilizer)], 0.03% magnesium oxide, 0.7% graphite
A-5 (explosive)	98.5% RDX, 1.5% stearic acid

A man-portable backpack LIBS system (MP-LIBS) has been developed by ARL with Ocean Optics, Inc. for field use (*15*). A small Nd:YAG laser is contained in a hand-held wand. The user holds the sensing wand with the laser and control stick near the sample. Colored filters surrounding the sample region act as splash guards and contain the laser beam in an enclosed area. The focusing optics and collection optics are also in the wand. The collected light from the LIBS plasma is delivered to a backpack spectrometer via a fiber optic cable. The data are then analyzed by an on-board computer and displayed in a heads-up display. The laptop and spectrometer fit into a backpack or suitcase, and the entire system weighs less than 20 lb.

A variety of LIBS spectra has previously been collected with the prototype unit shown in the upper left-hand corner of figure 3, ranging from plastic land mine casings to liquid chemical warfare simulants (*15*, *32–34*). For this study, single-shot spectra of RDX residue on an aluminum (Al) substrate (~400 ng/mm^2) were acquired with an MP-LIBS system with ~25 mJ

per laser pulse (1064 nm, ~7 ns). An argon flow was directed across the sample region, and 10 spectra each of the Al substrate and RDX were acquired. Air spectra were also obtained for comparison.

The laboratory double pulse LIBS system at ARL is shown in figure 4. Two Surelite* *Q*-switched Nd:YAG lasers are used to generate the two laser pulses. The pulses from each laser are delayed relative to one another by a Stanford Research pulse generator. When single pulse operation is desired, one 320-mJ laser pulse (1064 nm, 8 ns) is generated (the flashlamps continuously fire at 5 Hz). In double pulse mode, each pulse is 160 mJ and separated by 1 to 10 μs. The pulse train passes through a turning prism, a 100-mm focal length convex lens, and a pierced parabolic mirror. The emission from the plasma is collected by the parabolic mirror and focused onto the tip of a 600-μm fiber optic. The fiber is then inserted into a Catalina Scientific SE200† echelle spectrometer through a 25-micron pinhole. An intensified charge-coupled device (ICCD) serves as the detector. The intensified camera begins collecting spectra 2 μs after the initiation of the second plasma for 100 μs. An argon flow enables displacement of the air above the sample.

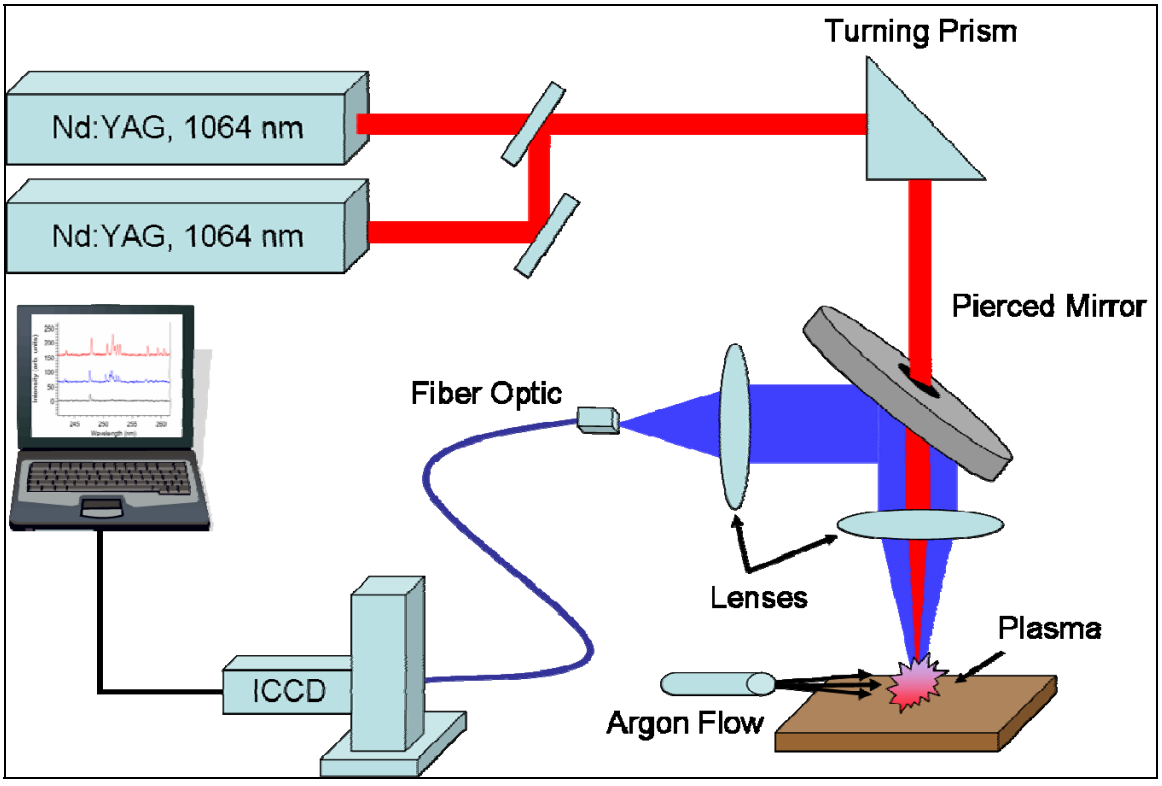

Figure 4. Laboratory double pulse LIBS experimental setup. (A 100-mm focal length convex lens is used to focus the Nd:YAG laser pulses on the sample surface. A 30-mm biconvex quartz lens focuses the plasma emission into the 600-μm fiber optic, which is sent to the spectrometer. An argon flow is positioned to eliminate the air above the sample surface.)

*Surelite is a trademark of Continuum; Continuum is a registered trademark.

†The SE200 is a designed and manufactured by Optomechanics Research Inc. and is protected by US patent 6,628,383.

LIBS spectra from the following samples were collected with the laboratory double pulse system: bulk Composition-B (Comp-B) (36% TNT, 63% RDX, and 1% wax), Comp-B residue on Al, bulk RDX, and RDX residue on Al. We prepared the residues by dissolving the explosive material in acetone for a concentration of 1 mg/mL. The solution was then deposited onto an Al substrate and allowed to evaporate. Spectra were collected in ambient atmosphere and under argon. Single-pulse LIBS spectra were collected from each sample under each bath gas. Double-pulse spectra were also collected under each gas at each of the interpulse delays ranging from 1 to 10 μs. Twenty spectra were collected of each sample for each experiment. A small amount of diesel fuel was spread onto an Al substrate in order to study the discrimination ability of single pulse LIBS relative to double pulse LIBS.

3. Results and Discussion

3.1 Initial Survey of Explosives and Energetic Materials

The initial survey of the explosives and energetic materials in table 1 resulted in the identification of the characteristic peaks observed in their LIBS spectra. Figure 5 presents a comparison of a pure air, RDX powder, and RDX pellet spectra. The nitrogen and oxygen signals in the RDX spectra are primarily from the entrainment of air into the laser-induced plasma, although the O/N ratio is noticeably higher in the RDX spectra. In addition to the nitrogen (N) (747, 821, and 869 nm) and oxygen (O) (777 and 844 nm) lines, the carbon (C) (247 nm) and hydrogen (H) (656 nm) lines are prevalent in the RDX spectra. The impurities magnesium (Mg) (279 and 285 nm), sodium (Na) (589 nm) and potassium (K) (766 and 769 nm) are also present in the explosives spectra. These lines can be attributed to the handling of the explosives or to the binders in operational explosives. The LIBS spectra of the different pure organic explosives are shown in figure 6. All share similar C, H, N, and O peaks.

LIBS spectra for the suite of operational explosives included in the study are shown in figure 7. From table 1, it can be seen that there is a diverse mixture of exotic components in these explosives because of the binders and plasticizers that they contain. The peaks that are attributable to C, H, N, and O in the organic explosives are observed, as are peaks attributable to the components of these secondary constituents. For example, Mg (279 and 285 nm) is identified in the JA2 and A-5 spectra. Calcium (Ca) (442, 558, 643 and 854 nm), Na, and K lines are also observed.

One possible way to extend LIBS as a practical approach to the detection and identification of explosives at an operational level is through spectral matching based on a predetermined and assembled spectral library of reference materials of interest. This approach would require the construction of a library of broadband spectra that would provide the basis for the comparison of the spectra for an unknown sample with those spectra contained in the library. The feasibility of

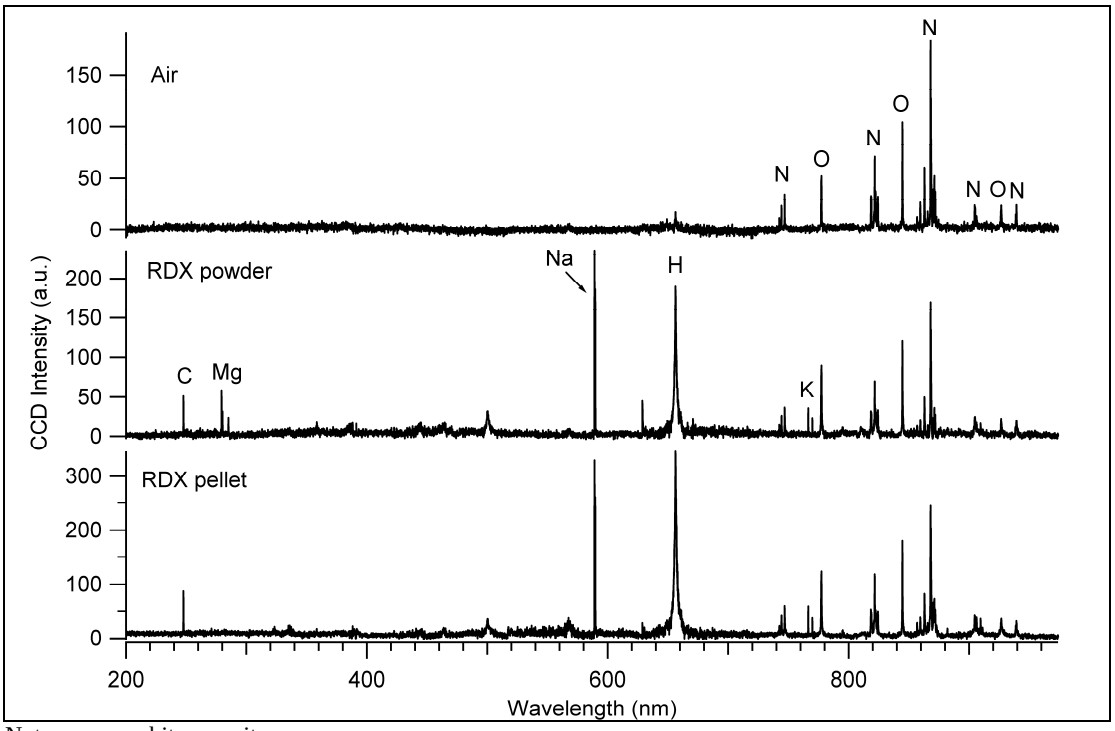

Note: a.u. = arbitrary units.

Figure 5. Representative single-shot LIBS spectra of an air spark, RDX powder, and an RDX pellet.

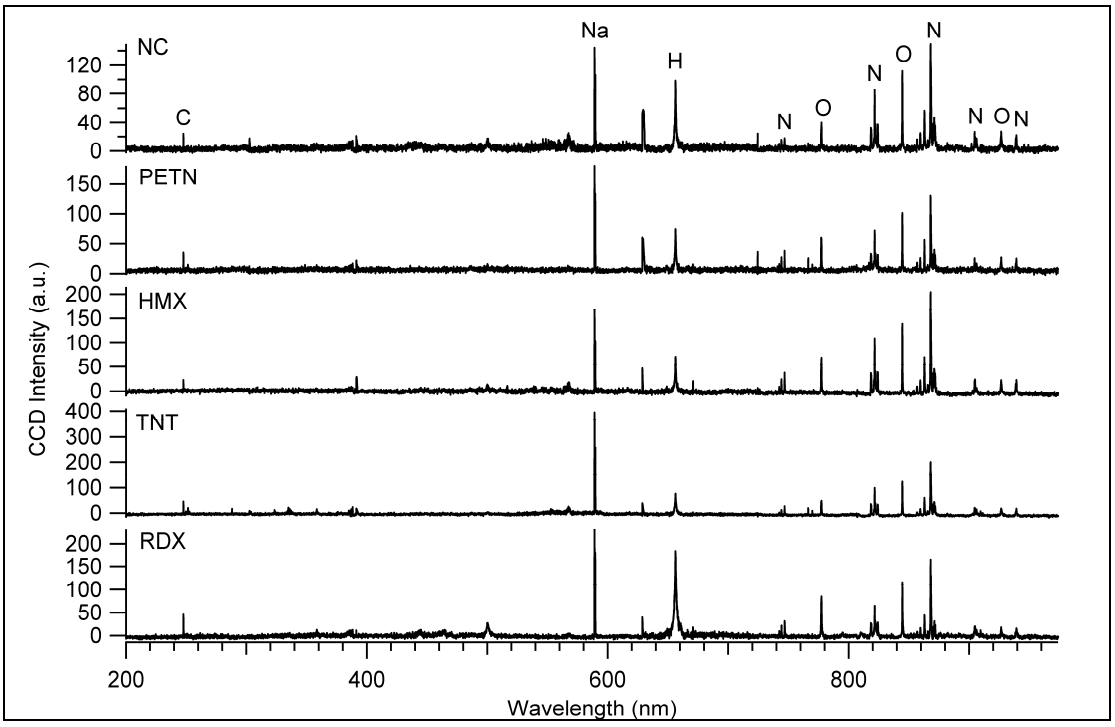

Figure 6. Single-shot LIBS spectra of pure energetic compounds: NC, PETN, HMX, TNT, and RDX.

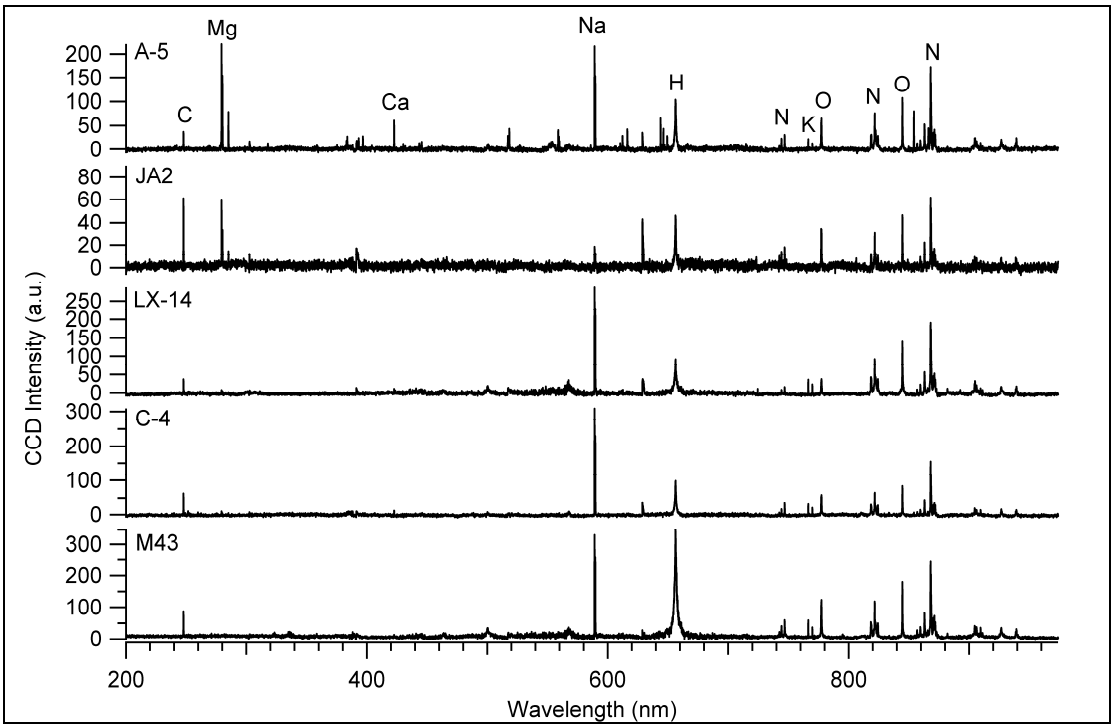

Figure 7. Single-shot LIBS spectra of several operational explosives and propellants: A-5, JA2, LX-14, C-4, and M43.

this approach was tested through the construction of a small library with the Ocean Optics software. By taking single-shot LIBS spectra of black powder and its principal components, we developed the library that included LIBS spectra of charcoal, a black powder pellet, sulfur, calcium sulfate, potassium nitrate, and ammonium nitrate. The LIBS spectrum of each of these component materials is shown in figure 8. We compared a series of single-shot LIBS spectra of a black powder pellet and powder with the library that we had constructed of black powder and its components. The library software identified the black powder and the black powder pellet as black powder in 150 of 150 tests. Charcoal, which is very similar in appearance to black powder, was identified as charcoal in 48 of 50 firings. Table 2 shows the results of several other comparisons.

The other approach to detection and identification of explosives is through the use of the stoichiometry of the compound for discrimination by the taking of a ratio of the elemental peaks of interest. A similar approach was explored by Anzano et al. to sort types of plastic (*18*). The intensity of the ratio of the C line at 247 nm to the H line at 656 nm was found to be different for each plastic. Whereas the LIBS spectra of all the plastics shared similar peaks, and the overall appearance of the LIBS spectra for the different plastics was highly similar, the peak intensity ratios of the elements were different to such an extent as to make differentiation of different plastic types possible. By analogy, it should be possible to identify the pure organic explosives in figure 6, based on differences in their stoichiometry (table 1).

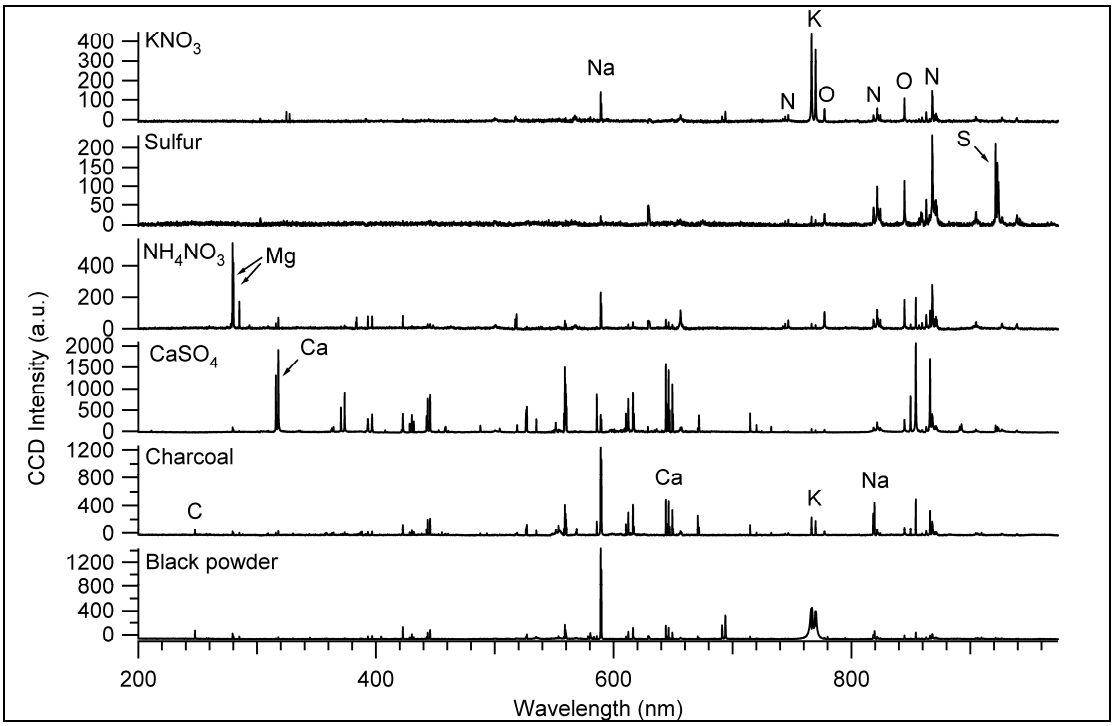

Figure 8. Single-shot LIBS spectra of black powder and its typical components: charcoal, calcium sulfate, ammonium nitrate, sulfur and potassium nitrate. (Strong lines of C, Mg, Na, N, K, O and S are labeled.)

Table 2. Results of LIBS spectra library comparison.

Sample	Correct Identifications (%)	No. of Tests
Black powder	100	150
Charcoal	96	50
KNO_3	94	50
$CaSO_4$	100	25

In addition to using the C:H peak intensity ratio, we might gain additional information from the O and N peak intensities. One concern that needs to be addressed is the interference of atmospheric N and O. A LIBS spectrum of air is shown in figure 5. Dry air includes ~80% N_2 and ~20% O_2. The ratio of the O peak at 777 nm to the N peak at 747 nm is 1.5. In figure 9, we compare RDX in air with RDX in argon (Ar). We have focused on the wavelength region from 600 to 800 nm to better observe the peaks of interest. The ratio of the O peak to the N peak from the LIBS spectrum of RDX in air is 2.5. This ratio is attributable to the intermixing of the O and N in RDX with O and N from air. Isolating the O and N in RDX by blowing Ar across the surface produces an interesting result. The formulation of RDX has equal amounts of O and N, a 1:1 ratio. Air alone has a 1:4 oxygen (20%) to nitrogen (80%) ratio. The LIBS peak O:N ratio in air is 1.5.

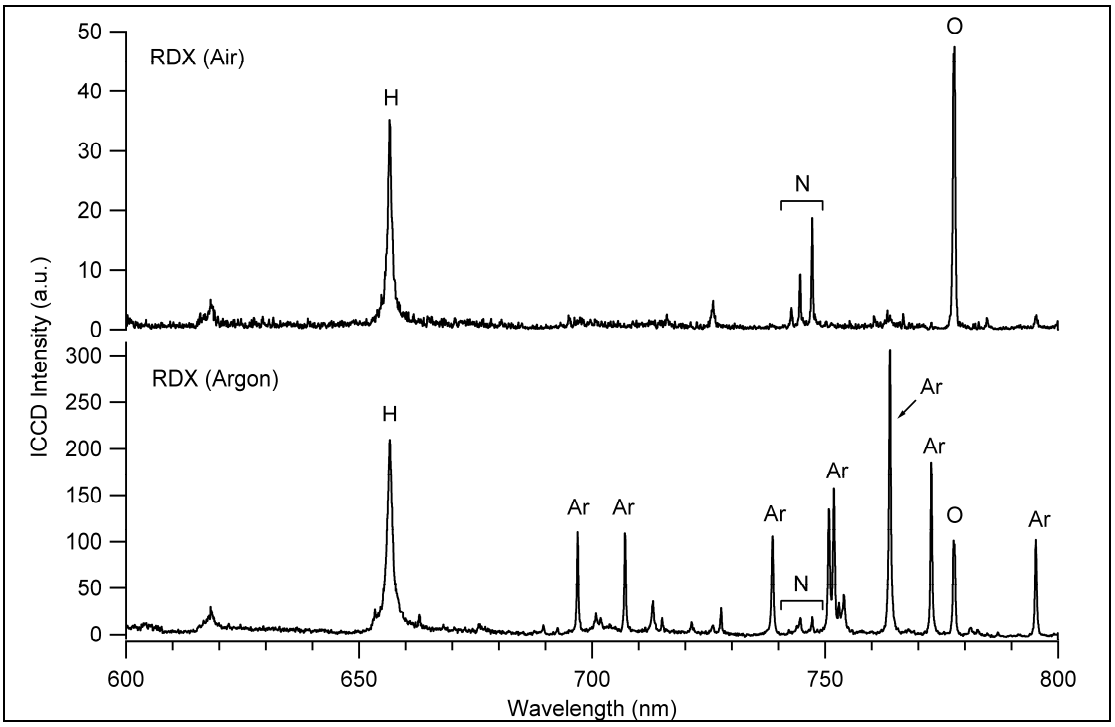

Figure 9. Single-shot LIBS spectra of RDX in air and in argon.

With a 1:1 O:N ratio, one would expect a LIBS peak ratio of four times a 1:4 O:N ratio. The LIBS peak ratio of RDX is therefore expected to be 6.0 because it has a 1:1 O:N ratio. In figure 9, the O:N LIBS peak intensity ratio is 5.6 for the RDX in Ar.

3.2 MP-LIBS Studies of Explosive Residues

The use of an argon flow to displace the air above the sample has also been tested with the MP-LIBS device. The single-shot spectra of RDX residue and Al acquired both in air and with an argon flow are shown in figure 10. The addition of argon to the LIBS plasma enhances the C (247 nm) and H (656 nm) lines, increasing the sensitivity of the MP-LIBS system. When argon is used to displace the air, the N (742, 744, and 747 nm) and O (777 nm) lines are representative of the sample composition rather than atmospheric contributions to the signal.

Figure 11 compares the peak intensity ratio of the oxygen to nitrogen for the four samples (Al in air, RDX on Al in air, Al in argon, and RDX on Al in argon). For the Al sample, O/N is indicative of the amount of oxygen relative to nitrogen in the atmosphere, since the sample itself contains no oxygen or nitrogen (except possibly from trace surface contamination). The RDX residue, on the other hand, contains more oxygen relative to nitrogen than air. The two samples cannot be discriminated based on the O/N value in air, but in argon, the decrease in the amount of air entrained in the plasma results in greater separation in the O/N values. These results show that for low pulse powers (single pulse), the use of argon is essential for improving the selectivity of the MP-LIBS system for explosive residue detection.

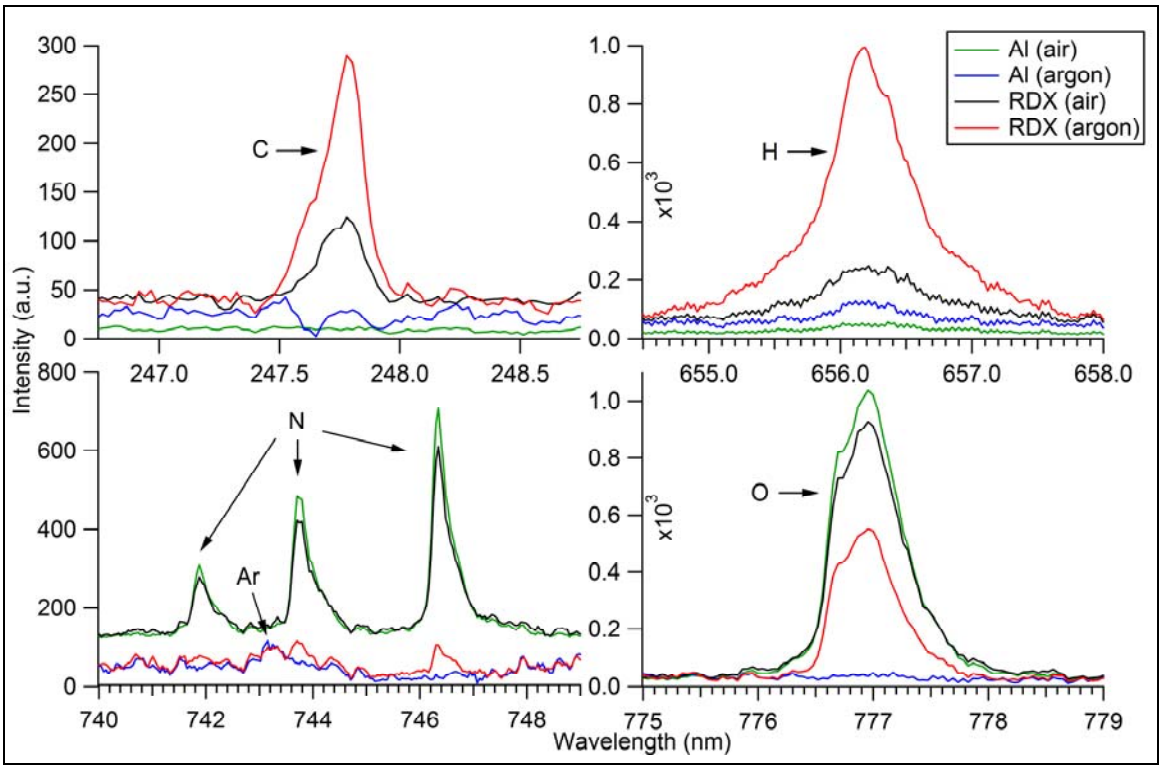

Figure 10. Single-shot spectra of Al and RDX residue on Al in air and under argon acquired with the MP-LIBS system. (Approximately 400 ng/mm^2 of RDX were applied to the Al foil substrate, and 10 spectra of each sample under each condition were acquired. The C [247 nm] and H [656 nm] signals from the RDX are enhanced under argon, while the O [777 nm] and N [742 to 747 nm] signals under argon are representative of the sample composition rather than atmospheric contributions.)

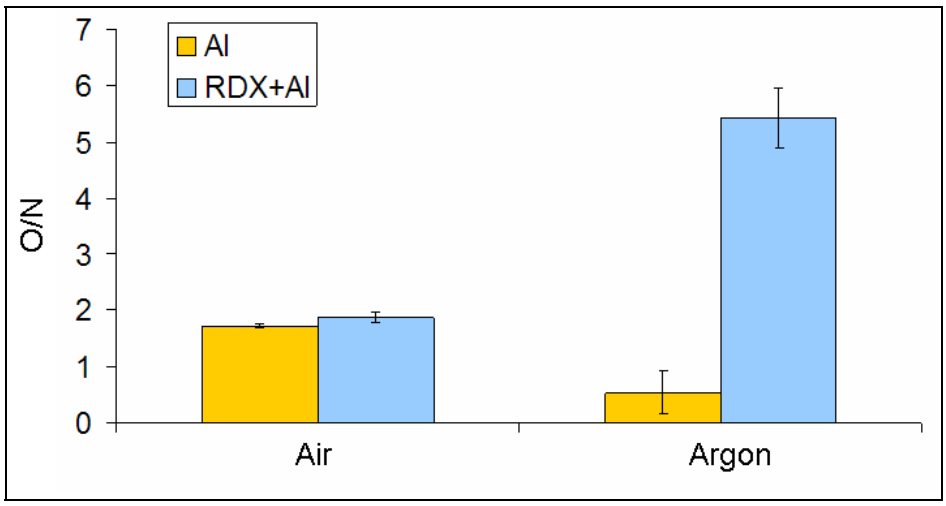

Figure 11. Relative oxygen to nitrogen peak intensities for Al and RDX residue on Al in air and in an argon flow (error bars represent ±σ for the 10 spectra acquired with the MP-LIBS system). (The RDX residue can only be discriminated from the Al substrate [with the O/N ratio] under argon.)

3.3 Laboratory Double Pulse LIBS Measurements of Explosives

We have investigated the use of argon as a buffer gas for explosive residue detection using higher laser powers with the laboratory double pulse LIBS system. Spectra were collected from samples in air and argon with double pulse (160 mJ/pulse) and single pulse (320 mJ/pulse) LIBS. Figure 12 compares the O/N ratios for each sample. The average O/N ratios for single pulse Al and RDX residue spectra in air overlap significantly as a result of the atmospheric contribution to the O and N signals. The use of an argon flow to displace the air results in a separation of the O/N values for the Al and RDX residue; this confirms the lower pulse energy MP-LIBS results (figure 11).

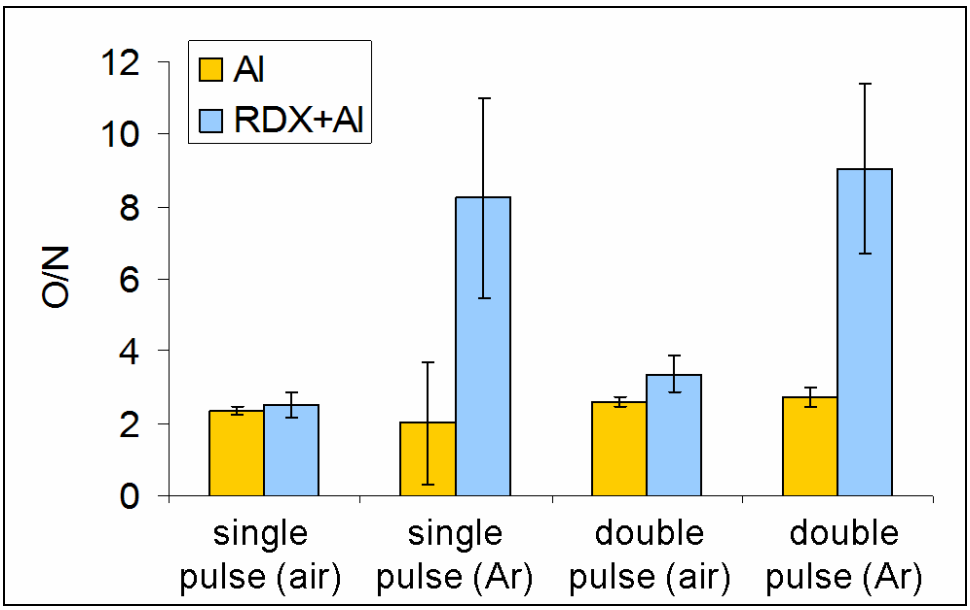

Figure 12. Comparison of the reduction in air entrainment with a single 320-mJ pulse under an argon flow versus using a double laser pulse (with an interpulse separation Δt=2 μs and total energy=320 mJ). (Twenty spectra of the Al and RDX residue samples in air and under an argon flow were acquired with the Continuum Surelite lasers in our laboratory LIBS setup. The oxygen-to-nitrogen ratios for a single 320-mJ pulse in air [maximum air entrainment] and a double-laser pulse under an argon flow [minimal air entrainment] are also shown for comparison. The Al and RDX residue can be discriminated, based on O/N when an argon flow and/or a double pulse is used, with the double pulse providing smaller standard deviations [i.e., the O/N values for the two samples do not overlap].)

Although these results confirm the necessity of using argon for single pulse LIBS detection of explosive residues, the ideal detector would be capable of stand-off detection of explosive residues from tens to hundreds of meters. An argon flow cannot practically be delivered to the sample surface for stand-off applications. As described in section 1.3, double pulse LIBS has been extensively investigated because of the signal enhancement attributable to the greater mass ablation and increase in plasma volume caused by the reduced density environment following the

first laser pulse. Figure 12 shows that separation of the O/N ratios for the Al and RDX samples can also be achieved with collinear double pulses. Although the separation between the samples is not as large as with the argon flow (since displacement of the air is not complete), the standard deviation of the measurements is significantly lower with double pulse. The combination of double pulse LIBS with an argon flow results in a large separation of the O/N ratios for the two samples, as well as lower standard deviations.

The carbon, hydrogen, nitrogen, and oxygen atomic emission lines from these spectra were used to determine if double pulse LIBS alone (with no argon flow) will minimize atmospheric oxygen and nitrogen interference sufficiently to enable the discrimination of energetic and non-energetic materials. Figure 13 compares a single pulse bulk RDX spectrum to the double pulse bulk RDX spectrum. The broadband spectra look almost identical, although a closer look at the regions of interest shows that analogous to the MP-LIBS air vs. argon study (figure 10), the C and H lines are enhanced with the double pulse while the O and N lines decrease. The differences in the key ratios for explosives (O/C, O/H, N/C, N/H, O/N) for single vs. double pulse shown in figure 14 follow the same trend observed with spectra obtained in air vs. argon. In other words, all the ratios decrease with double pulsing (and argon) except the O/N ratio, which increases. RDX residue, bulk Comp-B, and Comp-B residue also exhibit the same trend with double pulses. These results confirm that double pulse LIBS results in ratios indicative of the sample composition rather than the air entrained in the plasma.

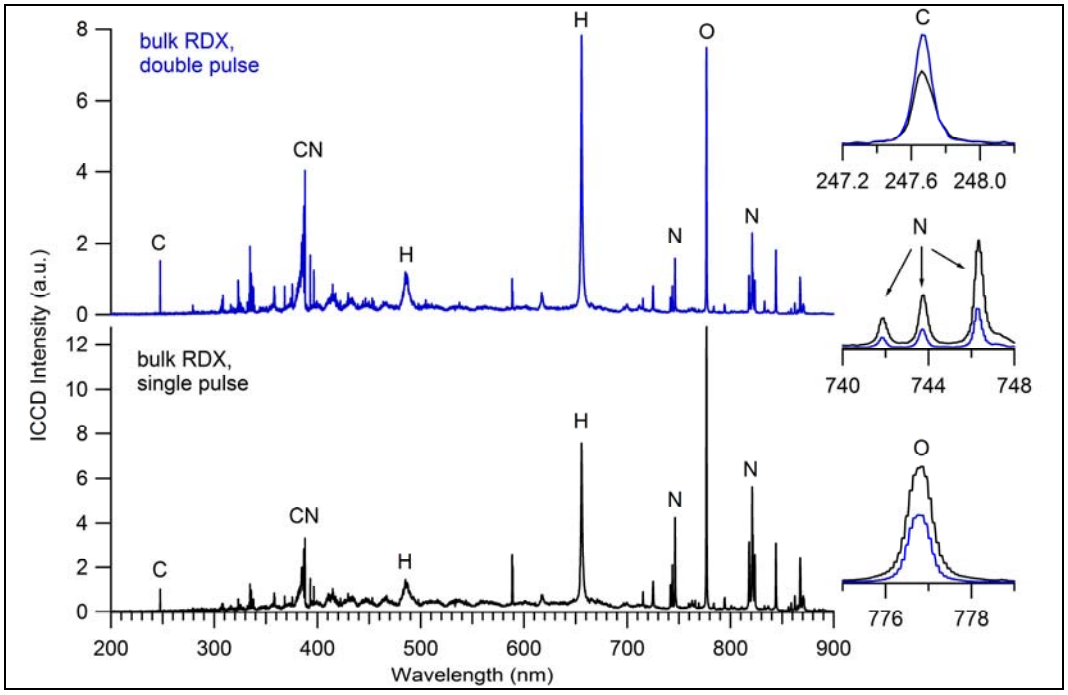

Figure 13. LIBS spectra of bulk RDX with a double laser pulse with Δt=2 μs (top) and a single laser pulse with equivalent pulse energy (bottom). (The carbon [inset right top] and hydrogen lines increase with double pulsing, while the nitrogen [inset right middle] and oxygen [inset right bottom] lines decrease because of the reduction in air entrained in the plasma.)

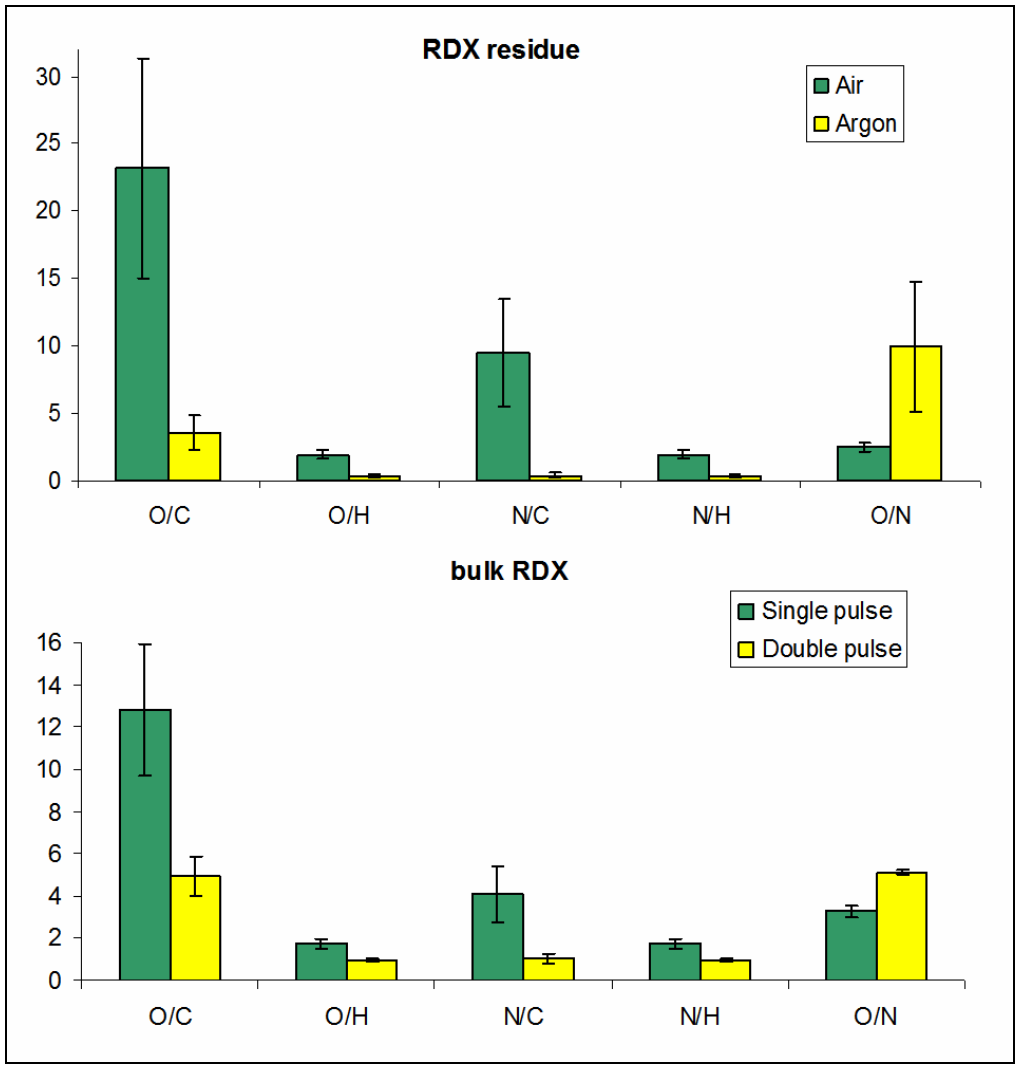

Figure 14. Peak atomic emission ratios from RDX residue on Al in air and in argon (top) and from bulk RDX with single pulse and double pulse (Δt=2 μs) LIBS (bottom). (The error bars represent one standard deviation. The same trend is observed in both cases, indicating that double pulse LIBS results in ratios indicative of the sample composition rather than the air entrained in the plasma.)

By comparing the oxygen-to-carbon atomic emission ratio of RDX residue from spectra collected at various delay times in air with the same ratios from spectra collected in argon, we can observe the effectiveness of double pulse LIBS in minimizing the influence of oxygen from the atmosphere on the spectra as a function of interpulse delay. Figure 15 shows the oxygen-to-carbon peak atomic emission ratios from an RDX residue on Al at a variety of interpulse delay times in air and argon. At Δt=0, corresponding to a single pulse with energy equal to the two pulses, the O/C ratio is much higher in air than argon, as observed in figure 14. As the single pulse is split into two pulses as an interpulse delay is introduced, the O/C ratio from the LIBS spectra collected in air decreases. By contrast, the O/C ratio from the spectra collected in argon with an interpulse delay remains fairly constant. The same trend is observed in the N/C, N/H,

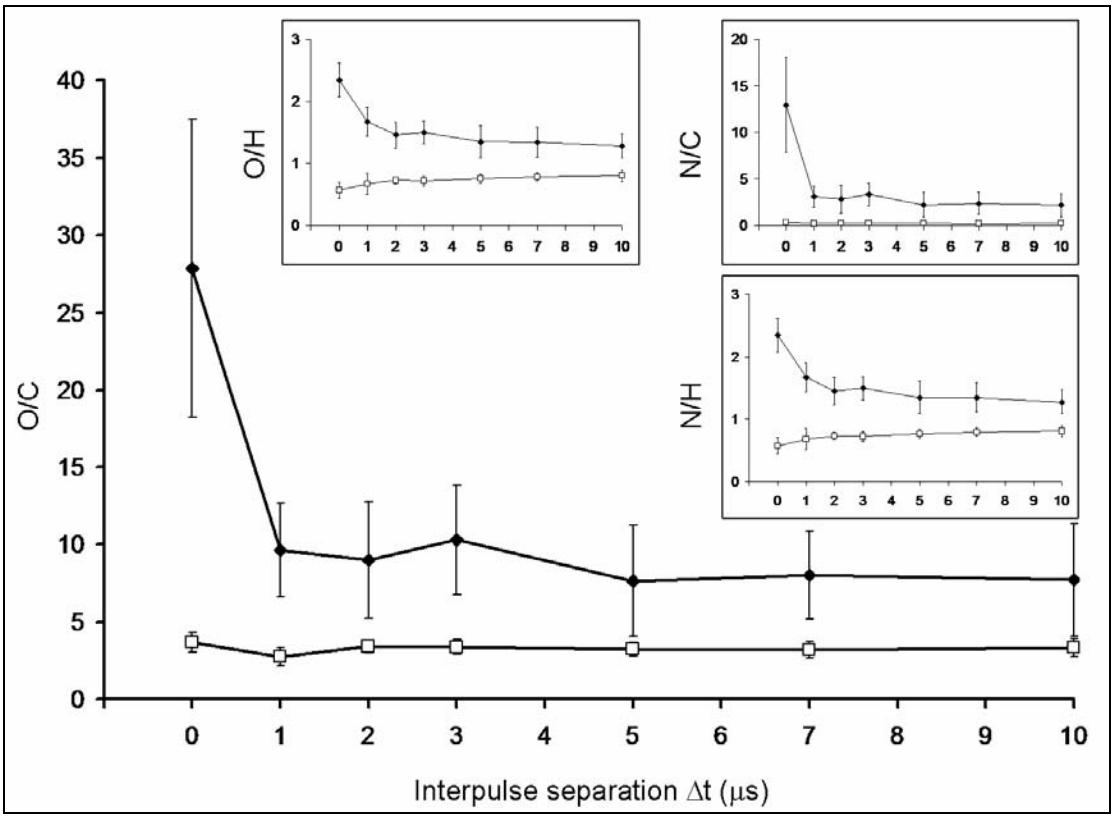

Figure 15. Peak atomic emission ratios of RDX residue on Al from various interpulse separation times (Δt) in argon (white square) and air (black diamond). (The ratios were calculated from 20 spectra collected at each Δt in both argon and air. The error bars represent one standard deviation.)

and O/H ratios shown in figure 15. The behavior is similar for all the samples: bulk Comp-B, bulk RDX, and Comp-B residue. The trend observed in figure 15 once again demonstrates that double pulse LIBS diminishes the oxygen and nitrogen from atmosphere. Of course, not all of the oxygen and nitrogen from the atmosphere are displaced by the double pulse. This is reflected in the fact that the emission ratios from double pulse LIBS spectra in air are larger than those in argon. However, the atomic emission ratio obtained from double pulse LIBS is much closer to the true ratio value of the sample than the ratio obtained from single pulse LIBS. Based on the decrease in the emission ratios and their standard deviations, an interpulse delay of 2 μs was chosen as the optimal timing for the detection of explosive residues with the laboratory double pulse LIBS system.

3.4 Discrimination of Energetic Materials With LIBS

In order to determine the ultimate utility of double pulse LIBS as a tool for explosives detection, it is important to test the discrimination between energetic and non-energetic organic materials. In this case, we collected LIBS spectra of diesel fuel residue and RDX residue, both on an Al substrate. Single pulse LIBS spectra were collected from each sample with a 320-mJ laser pulse. Double pulse LIBS spectra were collected from each sample with an interpulse separation of

2 μs and 160 mJ for each pulse. The peak atomic emission ratios, O/C, O/H, N/C, N/H, and O/N, were calculated from each spectrum collected. In order to compare the discrimination capability of double pulse LIBS to single pulse LIBS, we used the atomic emission ratios for each sample. The average O/C ratios from the single and double pulse LIBS spectra for RDX and diesel fuel are shown in figure 16. The RDX O/C ratio is larger than the O/C ratio from the diesel fuel in both cases. This result is expected since the amount of oxygen to carbon in RDX is higher than the amount of oxygen relative to carbon in diesel fuel (figure 1). However, the O/C ratio from the two samples overlaps within one standard deviation with single pulse LIBS. By contrast, the O/C ratio from the two samples does not overlap with double pulse LIBS.

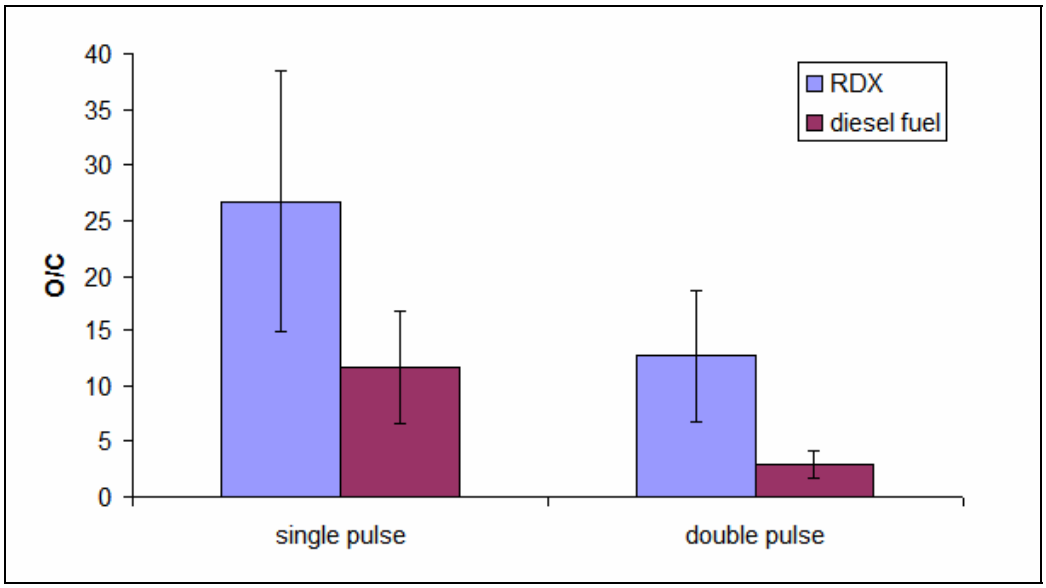

Figure 16. O/C peak atomic emission ration comparison of RDX and diesel fuel for single pulse and double pulse (Δt=2 μs) LIBS. (The error bars represent one standard deviation. The two samples can only be discriminated based on the O/C ratio by double pulse LIBS.)

A useful way to compare the effectiveness of discrimination methods is to use receiver operating characteristic (ROC) curves. A ROC curve measures the sensitivity of the detection versus specificity, i.e., the number of false alarms, in a two-member system. A threshold is established in order to categorize the unknown samples as one of the two members of the system. The threshold sweeps through all the values of the samples in order to create a ROC curve. An ideal ROC curve, i.e., complete discrimination between two samples, and the worst case for a ROC curve, i.e., a random predictor, are shown in figure 17.

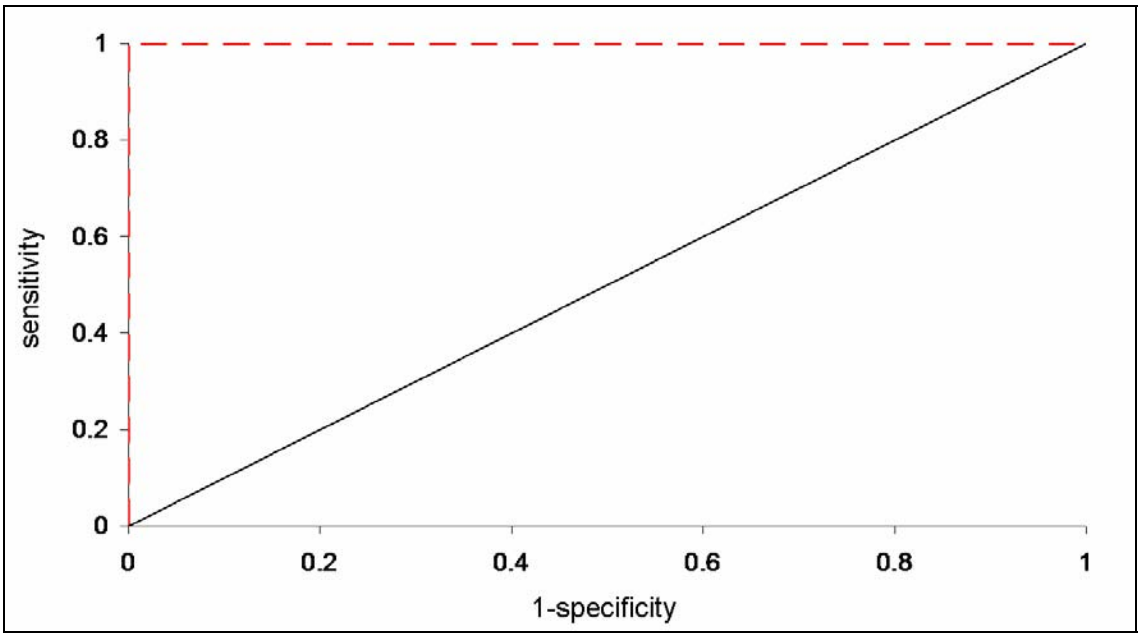

Figure 17. Examples of an ideal ROC curve (dashed line) and a ROC curve based on a random predictor (solid line).

In our case, the two members of our system are an energetic (RDX) and a non-energetic (diesel fuel). Our threshold for what is classified as an energetic is based on the value of the O/C ratio. Figure 18 shows the O/C ratio calculated from each individual spectrum collected with single pulse LIBS for the diesel fuel and the RDX residue. Everything above a certain O/C threshold is classified as an energetic material, while everything below it is classified as a non-energetic. The threshold was swept through all the O/C values calculated from spectra collected with single pulse LIBS in order to generate the solid ROC curve in figure 19. The circle indicates the point on the graph where 75% of the energetic RDX is identified with a false positive rate of 7%. In order to obtain >90% detection of RDX, the threshold is moved down on figure 18, and the position on the ROC curve follows the direction of the arrow. At this point, the false positive rate rises to 25%. Next, the O/C ratios from diesel fuel and RDX residue on Al were calculated from the spectra collected by double pulse LIBS. The threshold was swept through all the O/C ratios in order to generate a ROC curve based on data collected with double pulse LIBS. The ROC curve generated from these data is shown in figure 19. A comparison of the two ROC curves shows that the double pulse method improves discrimination. In order to obtain >90% detection of RDX in double pulse LIBS, the false positive rate is only 2.5% compared to 25% with single pulse LIBS. The double pulse LIBS minimizes the interference of atmospheric oxygen, more closely obtaining the true value of the O/C ratio of RDX and diesel fuel enhancing the discrimination.

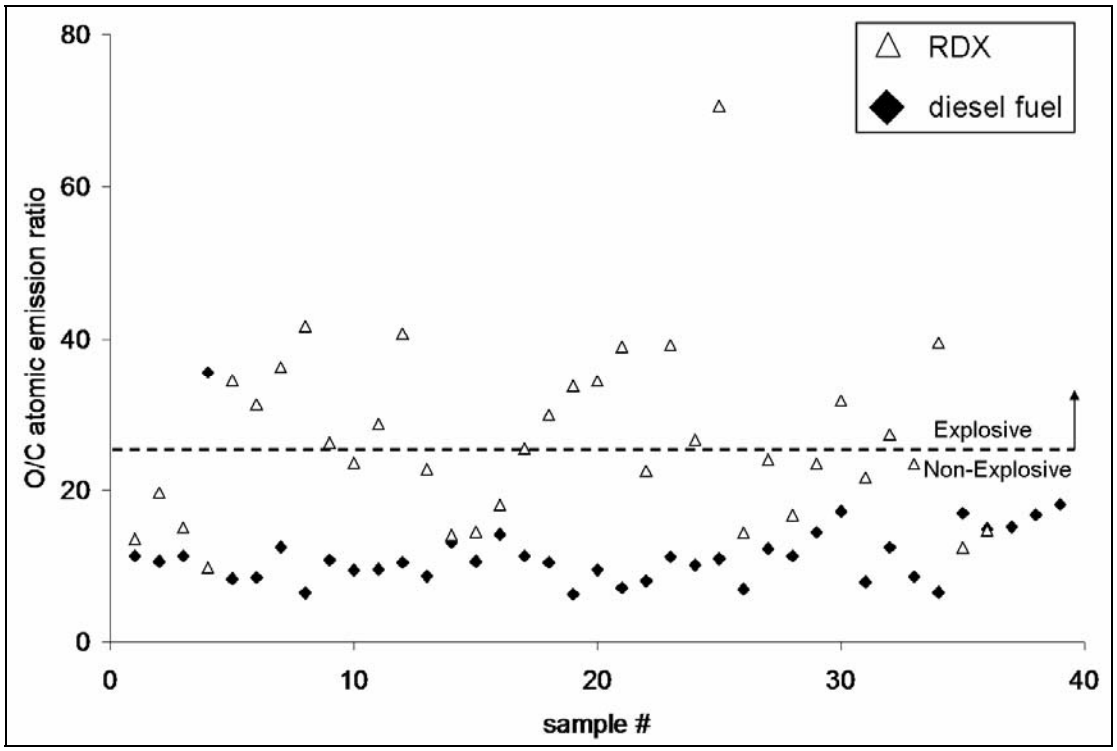

Figure 18. O/C peak atomic emission ratio for each single pulse LIBS spectrum taken of RDX residue and diesel fuel residue. (The dotted line represents the threshold that is moved along the y axis in order to create the ROC curve in figure 19.)

By combining LIBS data with principal components analysis (PCA), we have previously been able to discriminate between similar substances (*14*). PCA is a technique for simplifying a data set in order to ease analysis. It groups variables in the data and transforms them into principal components that describe the variance within the data. Instead of relying on one ratio, we can use all the atomic emission ratios associated with the energetic material calculated from the LIBS spectra (O/C, O/H, N/C, N/H, and O/N) can be used. Since most of the variance occurs in the first principal component (PC1) (>70%), we use the PC1 score values as the threshold to create our ROC curves. Figure 20 shows the scores for the first principal component for each sample, calculated from the five atomic emission ratios for each LIBS spectrum of RDX residue and diesel fuel by single pulse LIBS. Everything above the threshold is considered an energetic. The threshold is swept through the PC1 score values in order to generate the solid ROC curve in figure 21. The process is repeated for the LIBS spectra collected via double pulse LIBS in order to generate the dashed ROC curve in figure 21. Comparing the ROC curves in figure 19 generated from just one atomic emission ratio, O/C, with the ROC curves in figure 21 generated from PCA with the first principal component based on several atomic emission ratios, one can plainly see the improvement in discrimination. Furthermore, the data from the double pulse spectra in figure 21 represent the ideal ROC curve, 100% identification of RDX with 0% false positive rate.

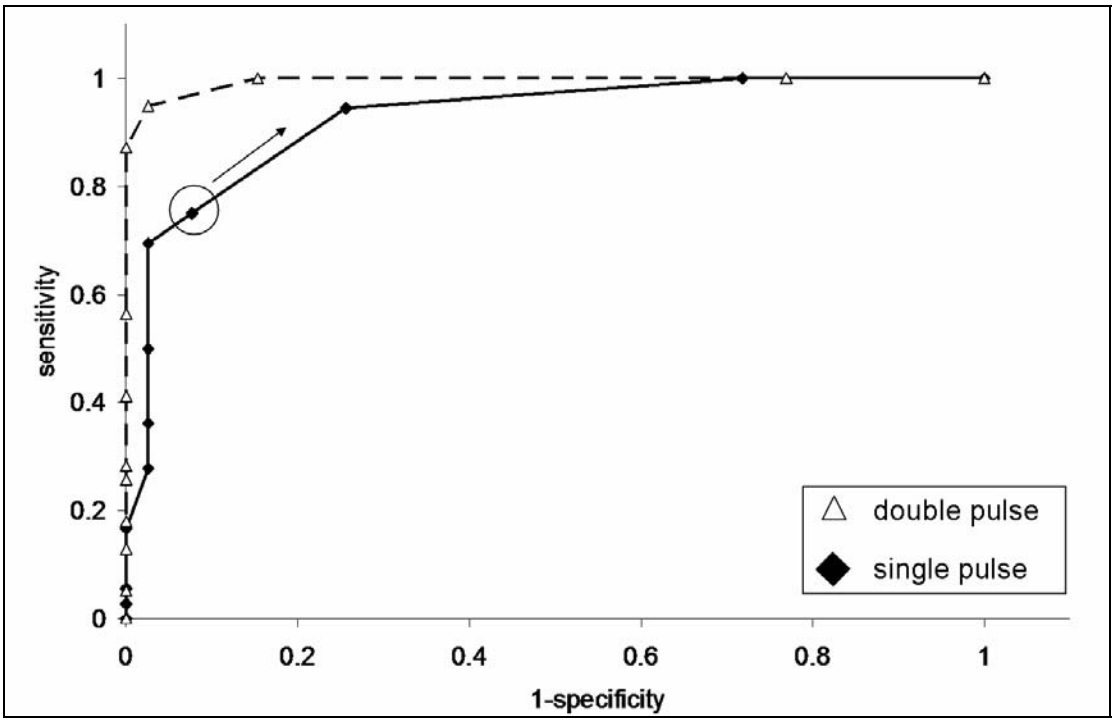

Figure 19. ROC curves created from O/C peak atomic emission ratios from single pulse and double pulse LIBS spectra of RDX and diesel fuel residues. (The circle represents a point on the ROC curve where 75% of the RDX samples are identified correctly as RDX and 7% of the diesel fuel samples are false positives [incorrectly identified as RDX]. Moving in the direction of the arrow increases the percentage of correct RDX identification but also increases the false positive rate. Moving this direction corresponds to lowering the threshold in figure 18. The ROC curve generated from the double pulse LIBS spectra is closer to an ideal predictor [figure 17].)

4. Conclusions

We have completed a LIBS survey of energetic materials and explosives, noting distinct differences between the inorganic explosive black powder and organic explosives; we also identified key elemental and molecular emission lines. In addition, we have tested the idea of using a broadband LIBS spectral library to identify an unknown explosive material (black powder) and its constituent components. Note that the laser-induced microplasma has never initiated detonation of any of the energetic materials that we have worked with because the short-lived spark provides an insufficient ignition source. However, we do expect detonation of materials that are especially shock sensitive as well as ignition of reactive gaseous mixtures.

In order to better discriminate energetic material from non-energetic material, interference from atmospheric nitrogen and oxygen must be minimized. Two methods for diminishing the atmospheric interference have been studied: displacing the atmosphere with an inert gas and

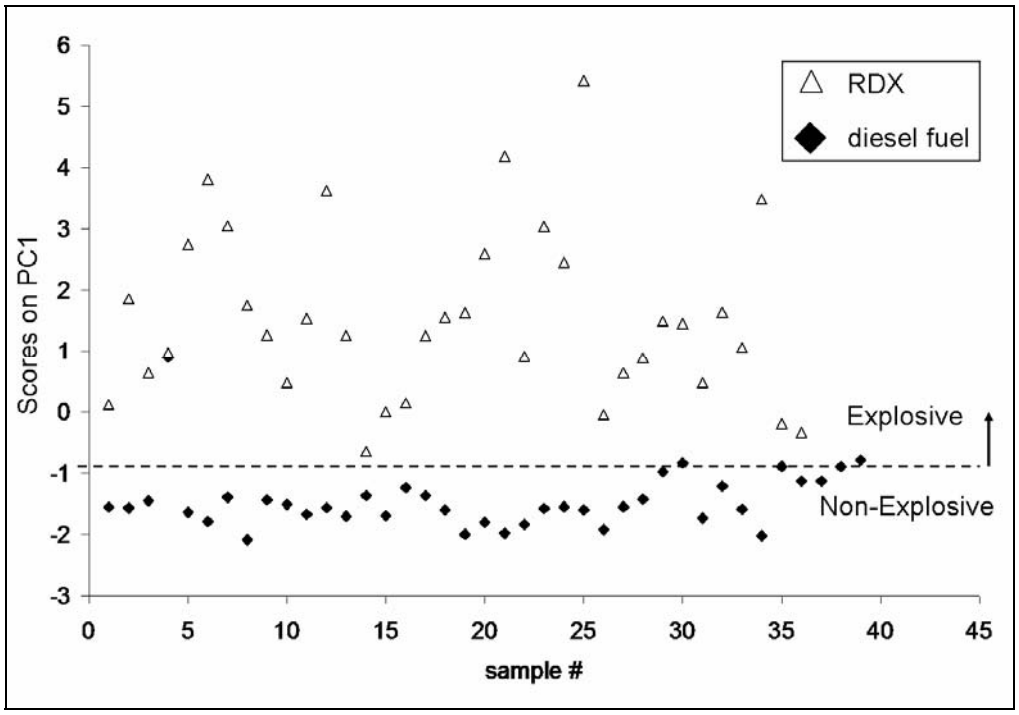

Figure 20. First principal component from atomic emission ratios O/C, O/H, N/C, N/H, and O/N from each single pulse LIBS spectrum of RDX and diesel fuel residue. (The dotted line represents the threshold that is moved along the y axis in order to create the ROC curve in figure 21.)

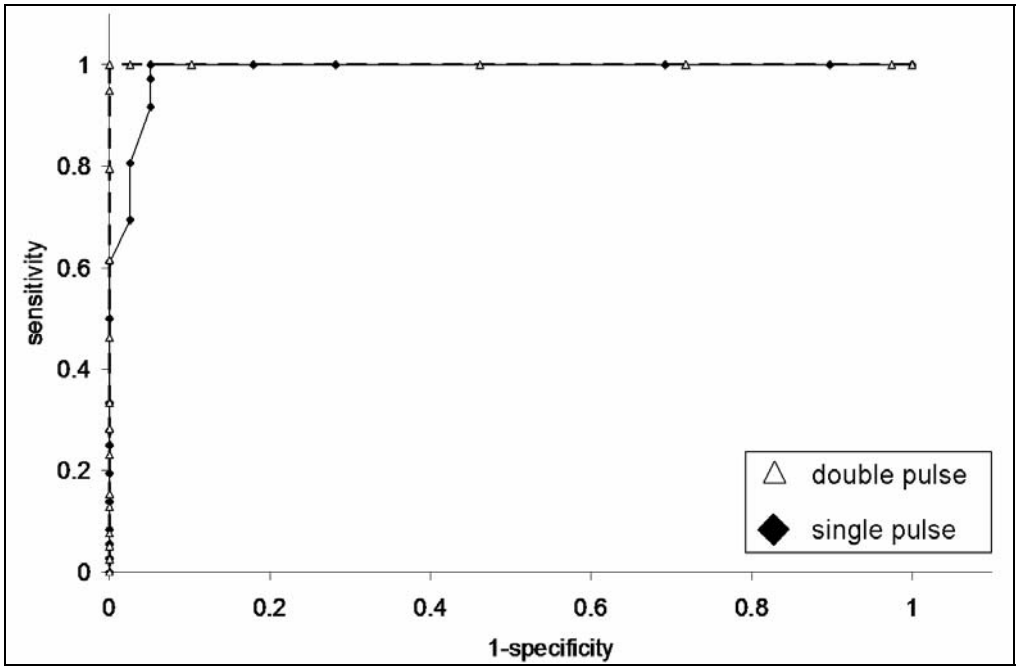

Figure 21. ROC curves created from the first principal component calculated from atomic emission ratios from single pulse and double pulse LIBS spectra of RDX and diesel fuel residue in figure 20. (The double pulse ROC curve represents complete separation between RDX and diesel fuel residue [100% correct identification].)

double pulse LIBS. Displacing the surrounding atmosphere with argon eliminates all atmospheric nitrogen and oxygen. The nitrogen and oxygen atomic emission lines in the LIBS spectra collected from samples under argon are characteristic of the material composition. We have also investigated the capability of double pulse LIBS to minimize the oxygen and the nitrogen from the surrounding atmosphere, since delivering an argon flow to the sample surface at stand-off distances (tens of meters) would be impractical.

The double pulse LIBS spectra have been shown to effectively diminish the interference of atmospheric oxygen and nitrogen because of the decrease in gas density caused by the first laser pulse (*28–31*). Thus, the oxygen and nitrogen from the atmosphere do not interfere with the LIBS signal of the sample. Using ROC curves and PCA, we have shown that double pulse LIBS improves the discrimination between an energetic sample (RDX residue) and a non-energetic sample (diesel fuel). The double pulse technique, although not quite as effective as displacing the atmosphere with an inert gas in order to minimize atmospheric oxygen and nitrogen interference, has the advantage of being applicable to a stand-off LIBS system. An ensuing report (*17*) will discuss the extension of the techniques described here to stand-off distances and will present more advanced chemometric techniques to improve the selectivity of LIBS for explosives detection.

5. References

1. McNesby, K. L.; Pesce-Rodriguez, R. A. Applications of Vibrational Spectroscopy in the Study of Explosives. In *Handbook of Vibrational Spectroscopy*; Chalmers, J. M., Griffiths, P. R., Eds.; Wiley: Chichester, England, 2002.
2. Detection of Explosives for Commercial Aviation Security, National Research Council Committee on Commercial Aviation Security, Commission on Engineering and Technical Systems (National Academies Press). http://www.nap.edu/catalog/2107.html. 1993
3. Parmeter, J. E. The Challenge of Standoff Explosives Detection. *38th Annual International Carnahan Conference on Security Technology*, 2004, pp 355–358, (doi: 10.1109/CCST .2004.1405418).
4. Federici, J. F.; Schulkin, B.; Huang, F.; Gary1, D.; Barat, R.; Oliveira, F.; Zimdars, D. THz Imaging and Sensing for Security Applications—Explosives, Weapons and Drugs. *Semicond. Sci. Technol*. **2005**, *20*, S266–S280.
5. Munson, C. A.; Gottfried, J. L.; De Lucia, F. C. Jr.; McNesby, K. L.; Miziolek, A. W. Laser-Based Detection Methods of Explosives. In Counterterrorist Detection Techniques of Explosives, J. Yinon, Ed.; Elsevier: Amsterdam, 2007, pp 279–321.
6. Steinfeld, J. I.; Wormhoudt, J. Explosives Detection: A Challenge for Physical Chemistry, *Annu. Rev. Phys. Chem.* **1998**, *49*, 203–232.
7. Gresham, G. L.; Davies, J. P.; Goodrich, L. D.; Blackwood, L. G.; Liu, B. Y. H.; Thimsem, D.; Yoo, S. H.; Hallowell, S. F. Development of Particle Standards for Testing Detection Systems: Mass of RDX and Particle Size Distribution of Composition 4 Residues. *Proc. SPIE-Int. Soc. Opt. Eng.* 1994, *2276*, 34–44.
8. Sharma, S. K.; Misra, A. K.; Sharma, B. Portable Remote Raman System for Monitoring Hydrocarbon, Gas Hydrates and Explosives in the Environment. *Spectrochimica Acta, Part A* 2005, *61*, 2404–2412.
9. Carter, J. C.; Angel, S. M.; Lawrence-Snyder, M.; Scaffidi, J.; Whipple, R. E.; Reynolds, J. G. Standoff Detection of High Explosive Materials at 50 Meters in Ambient Light Conditions Using a Small Raman Instrument. *Appl. Spectrosc.* 2005, *59*, 769–775.
10. Rusak, D. A.; Castle, B. C.; Smith, B. W.; Winefordner, J. D. Fundamentals and Applications of Laser-Induced Breakdown Spectroscopy. *Crit. Rev. Anal. Chem.* 1997, *27*, 257–290; Miziolek, A.; Palleschi, V.; Schechter, I., Eds.; Laser Induced Breakdown Spectroscopy; Cambridge University Press: Cambridge, UK, 2006.

11. Williamson, C. K.; McNesby, K. L.; Daniel, R. G.; Miziolek, A. W. Laser-Induced Breakdown Spectroscopy for Real-Time Detection of Halon Alternative Agents. *Anal. Chem*. 1998, *70*, 1186–1191.

12. Wainner, R. T.; Harmon, R. S.; Miziolek, A. W.; McNesby, K. L.; French, P. D. Analysis of Environmental Lead Contamination: Comparison of LIBS Field and Laboratory Instruments. *Spectrochim. Acta Part B* 2001, *56***,** 777–793.

13. Samuels, A. C.; De Lucia, Jr. F. C.; McNesby, K. L.; Miziolek, A. W. Laser-Induced Breakdown Spectroscopy of Bacterial Spores, Molds, Pollens, and Protein: Initial Studies of Discrimination Potential. *Appl. Opt.* 2003, *42*, 6205–6209.

14. Munson, C. A.; De Lucia, Jr., F. C.; Piehler, T.; McNesby, K. L.; Miziolek, A. W. Investigation of Statistics Strategies for Improving the Discriminating Power of Laser-Induced Breakdown Spectroscopy for Chemical and Biological Warfare Agent Simulants. *Spectrochim. Acta, Part B* 2005, *60*, 1217–1224.

15. De Lucia, Jr., F. C.; Samuels, A. C.; Harmon, R. S.; Walters, R. A.; McNesby, K. L.; LaPointe, A.; Winkel, Jr., R. J.; Miziolek, A. W. Laser-Induced Breakdown Spectroscopy (LIBS): A Promising Versatile Chemical Sensor Technology for Hazardous Material Detection. *IEEE Sensors Journal* 2005, *5***,** 681–689.

16. Gottfried, J. L.; De Lucia, Jr., F. C.; Munson, C. A.; Miziolek, A. W. Double-Pulse Standoff Laser-Induced Breakdown Spectroscopy (ST-LIBS) for Versatile Hazardous Materials Detection. *Spectrochim. Acta, Part B*, submitted for the LIBS2006 special issue.

17. Gottfried, J. L.; De Lucia Jr., F. C.; Munson, C. A.; Ford, C.; Miziolek, A. W. *Detection of Energetic Materials and Explosive Residues With Laser-Induced Breakdown Spectroscopy: II. Standoff Measurements*; ARL-TR-4241;U.S. Army Research Laboratory: Aberdeen Proving Ground, MD, 2007.

18. Anzano, J. M.; Gornushkin, I. B.; Smith, B. W.; Winefordner, J. D. Laser-Induced Plasma Spectroscopy for Plastic Identification. *Polym. Eng. Sci.* 2000, *40*, 2423–2429.

19. Portnov, A.; Rosenwaks, S.; Bar, I. Emission Following Laser-Induced Breakdown Spectroscopy of Organic Compounds in Ambient Air. *Appl. Opt.* 2003, *42*, 2835–2842.

20. Ferioli, F.; Buckley, S. G. Measurements of Hydrocarbons Using Laser-Induced Breakdown Spectroscopy. *Combust. Flame* 2006, *144*, 435–447.

21. Tran, M.; Sun, S.; Smith, B. W.; Winefordner, J. D. Determination of C:H:O:N Ratios in Solid Organic Compounds by Laser-Induced Plasma Spectroscopy. *J. Anal. At. Spectrom.* 2001, *16*, 628–632.

22. Existing and Potential Standoff Explosives Detection Techniques, Washington D.C., Committee on the Review of Existing and Potential Standoff Explosives Detection Techniques, National Research Council. http://www.nap.edu /catalog /10998.html (accessed 7 May 2007, published 2004).

23. Yinon, J. *Forensic and Environmental Detection of Explosives*; Wiley and Sons: Chichester, UK, 1999.

24. De Lucia, Jr., F. C.; Harmon, R. S.; McNesby, K. L.; Winkel, Jr., R. J.; Miziolek, A. W. Laser-Induced Breakdown Spectroscopy Analysis of Energetic Materials. *Appl. Opt.* 2003, *42*, 6148–6152.

25. Lee, Y. -L.; Thiem, T. L.; Kim, G. -H.; Teng, Y. -Y.; Sneddon, J. Interaction of an Excimer-Laser Beam with Metals. Part III: The Effect of a Controlled Atmosphere in Laser-Ablated Plasma Emission. *Appl. Spectrosc.* 1992, *46*, 1597–1604.

26. Stratis, D.; Eland, K.; Angel, S. Dual-Pulse LIBS Using a Pre-Ablation Spark for Enhanced Ablation And Emission. *Appl. Spectrosc.* 2000, *54*, 1270–1274.

27. Angel, S. M.; Stratis, D. N.; Eland, K. L.; Lai, T.; Berg, M. A.; Gold, D. M. LIBS Using Dual-and Ultra-Short Laser Pulses. *Fresen. J. Anal. Chem.* 2001, *369*, 320–327.

28. Corsi, M.; Cristoforetti, G.; Giuffrida, M.; Hidalgo, M.; Legnaioli, S.; Palleschi, V.; Salvetti, A.; Tognoni, E.; Vallebona, C. Three-Dimensional Analysis of Laser Induced Plasmas in Single and Double Pulse Configuration. *Spectrochim. Acta, Part B* 2004, *59*, 723–735.

29. Gautier, C.; Fichet, P.; Menut, D.; Lacour, J.; L'Hermite, D.; Dubessy, J. Main Parameters Influencing the Double-Pulse Laser-Induced Breakdown Spectroscopy in the Collinear Beam Geometry. *Spectrochim. Acta, Part B* 2005, *60*, 792–804.

30. Scaffidi, J.; Angel, S.; Cremers, D. Emission Enhancement Mechanisms in Dual-Pulse LIBS. *Anal. Chem.* 2006, *78*, 24–32.

31. Babushok, V. I.; DeLucia Jr., F. C.; Gottfried, J. L.; Munson, C. A.; Miziolek, A. W. Double-Pulse Laser Ablation and Plasma: LIBS Signal Enhancement. *Spectrochim. Acta, Part B*, 2006, *61*, 999–1014.

32. Harmon, R. S.; De Lucia, Jr., F. C.; Munson, C. A.; Miziolek, A. W.; McNesby, K. L. Laser-Induced Breakdown Spectroscopy (LIBS): An Emerging Field-Portable Sensor Technology for Real-Time Chemical Analysis for Military, Security and Environmental Applications. *Proc. SPIE-Int. Soc. Opt. Eng.* 2005, *5994*, 59940K/1–7.

33. Harmon, R. S.; De Lucia, Jr., F. C.; LaPointe, A.; Winkle, Jr., R. J.; Miziolek, A. W. LIBS for Landmine Detection and Discrimination. *Anal. Bioanal. Chem.* 2006, *385*, 1140–1148.

34. Harmon, R. S.; De Lucia, Jr., F. C.; LaPointe, A.; Miziolek, A. W. Man-portable LIBS for Landmine Detection. *Proc. SPIE-Int. Soc. Opt. Eng.* 2006, *6217*, 62140I/1–7.

NO. OF COPIES	ORGANIZATION
1 (PDF ONLY)	DEFENSE TECHNICAL INFORMATION CTR DTIC OCA 8725 JOHN J KINGMAN RD STE 0944 FORT BELVOIR VA 22060-6218
1	US ARMY RSRCH DEV & ENGRG CMD SYSTEMS OF SYSTEMS INTEGRATION AMSRD SS T 6000 6TH ST STE 100 FORT BELVOIR VA 22060-5608
1	DIRECTOR US ARMY RESEARCH LAB IMNE ALC IMS 2800 POWDER MILL RD ADELPHI MD 20783-1197
3	DIRECTOR US ARMY RESEARCH LAB AMSRD ARL CI OK TL 2800 POWDER MILL RD ADELPHI MD 20783-1197

ABERDEEN PROVING GROUND

1	DIR USARL AMSRD ARL CI OK TP (BLDG 4600)

NO. OF COPIES ORGANIZATION

2 DIR USARL
AMSRD ARL SE EO
P PELLIGRINO
D STRATIS-CULLUM
2800 POWDER MILL ROAD
ADELPHI MD 20783-1197

3 BATTELLE EASTERN SCI & TECHNLGY CTR
C W MULLINS
B W JEZEK
A ELLIS
1204 TECHNOLOGY DR
ABERDEEN MD 21001-1228

2 NIGHT VISION AND ELECT SENSORS DIR
A LAPOINTE
K SHIRBANDI
10221 BURBECK RD
FT BELVOIR VA 22060

1 OFC OF THE SECRETARY OF DEFENSE
G A FOGG
2231 CRYSTAL DR
STE 900
ARLINGTON VA 22202

1 CHEMIMAGE
PATRICK J TREADO
7301 PENN AVE
PITTSBURGH PA 15208

1 A3 TECHNOLOGIES LLC
RICK RUSSO
PO BOX 5049
WALNUT CREEK CA 94596

1 BAE SYSTEMS
J F ERDMANN
TECHNLGY SOLUTIONS SECTOR
SYSTEMS ENGINEERING SOLUTIONS
PO BOX 381
DAHLGREN VA 22448-0381

1 WHITING SCHOOL OF ENGRG
MARC D DONAHUE
120 NEW ENGINEERING BLDG
3400 N CHARLES ST
BALTIMORE MD 21218-2681

NO. OF COPIES ORGANIZATION

1 IDAHO NATIONAL LAB
E CESPEDES
PO BOX 1625
IDAHO FALLS ID 83415-3690

1 TRANSPORTATION SECURITY LAB
OFC OF RSRCH AND DEV
RICHARD T LAREAU
BLDG 315 TSL-200
ATLANTIC CITY
INTERNATIONAL AIRPORT NJ 08405

1 NATL CENTER FOR FORENSIC SCI
M E SIGMAN
UNIV OF CENTRAL FLORIDA
PO BOX 162367
ORLANDO FL 32816-2367

1 MATERIALS DYNAMICS GROUP
D S MOORE
DYNAMIC EXPERIMENTATION DIV
MAILSTOP P952
LOS ALAMOS NM 87545

1 ATSE DOT CM
D D DIETZ
320 MANSCEN LOOP STE 115
FT LEONARD WOOD MO 65473-8929

1 RAPID EQUIPPING FORCE
J GEDDES
10236 BURBECK RD
FT BELVOIR VA 22060-5852

1 US DEPT OF HOMELAND SECURITY
SCI AND TECHLGY
M SHEPARD
WASHINGTON DC 20528

1 G GILBERT
MCMR ZB T
504 SCOTT ST
FT DETRICK MD 21702-5012

1 MENTIS SCIENCES
J PLUMER
150 DOW ST
TOWER TWO
MANCHESTER NH 03101

NO. OF COPIES ORGANIZATION

1 DEPT OF PHYSICS USMA
COL R WINKEL
WEST POINT NY 10996-1790

1 US ARMY RESEARCH OFC
R HARMON
4300 S MIAMI BLVD
DURHAM NC 27709-2211

1 ENVIMETRICS INC
P EFTHIMION
PO BOX 6
PLUCKEMIN NJ 07978

1 APPLIED RSRCH ASSOCIATES INC
C N NORTHRUP
2672 BAYSHORE PARKWAY
STE 1035
MOUNTAIN VIEW CA 94043

1 SANDIA NATIONAL LAB
CONTRABAND DETECTION
L THEISEN
PO BOX 5800 MS0782
ALBUQUERQUE NM 87185-0782

1 PENNSYLVANIA STATE UNIV
APPLIED RSRCH LAB
D MERDES
PO BOX 30
STATE COLLEGE PA 16804-0030

1 ENERGY RESEARCH COMPANY
R DE SARO
2571-A ARTHUR KILL RD
STATEN ISLAND NY 10309

1 HAMILTON SUNDSTRAND
S COMBS
2771 NORTH GAREY AV
POMONA CA 91767

1 AMERICAN MEASUREMENT
SOLUTIONS
T MARLOW
1 CORAL BELL COURT
SANTA FE NM 87508

NO. OF COPIES ORGANIZATION

ABERDEEN PROVING GROUND

1 A W FOUNTAIN III
AMSRD ECB RT D
BLDG E3330/147
APG EDGEWOOD MD 21010-5424

2 USAATC
CSTE DTC AT SL F
C SIMPSON
W BOLT
BLDG 451
400 COLLERAN RD
APG MD 21005-5059

1 CAMBER CORP
GARY SCHEFFLER
5183 BLACKHAWK RD
BLDG E3549
APG MD 21010-5424

18 DIR USARL
AMSRD ARL WM B
M ZOLTOSKI
MAJ C FORD
J MORRIS
AMSRD ARL WM BD
S PIRAINO
R PESCE-RODRIGUEZ
R SAUSA
F DELUCIA JR
A MIZIOLEK
P KASTE
B FORCH
J GOTTFRIED
M GRAMS
K MCNESBY
R BEYER
B RICE
B HOMAN
J NEWBERRY
C MUNSON

NO. OF
COPIES ORGANIZATION

1 A WHITEHOUSE
APPLIED PHOTONICS LIMITED
UNIT 8 CARLETON BUSINESS PARK
SKIPTON NORTH YORKSHIRE
BD23 2DE UNITED KINGDOM

INTENTIONALLY LEFT BLANK.